ASSESSING THE ROLE OF KERATIN 17 IN THE DNA DAMAGE RESPONSE *IN VIVO*

by

Stefan Alexander Prendergast

A thesis submitted to Johns Hopkins University in conformity with the requirements for the degree of Master of Science

Baltimore, Maryland

August 2016

© 2016 Stefan Prendergast
All Rights Reserved

ABSTRACT

The type I intermediate filament protein keratin 17 (K17) is normally absent in the interfollicular epidermis but is robustly induced in the setting of inflammatory skin disorders such as psoriasis and cancer. Our recent research indicated that genetic loss of *Krt17* results in a delayed onset of tumor development correlating with reduced expression of pro-inflammatory genes and attenuated inflammation in mouse models for basal cell carcinoma (*Gli2*-transgenic) and squamous cell carcinoma (HPV16-transgenic). However, no effort has yet been made to define the role of keratins in the specific stages of carcinogenesis, in particular in the initial oncogenic stresses that lead to subsequent tumor development. Herein, we sought to elucidate whether K17 expression is responsive to DNA damage, and if the presence or absence of K17 would alter the DNA damage response.

Using immunofluorescence microscopy, Western blotting and qRT-PCR, we assessed the DNA damage response in HPV16$^{Tg/+}$ mice at postnatal day 50 (P50) in the presence or absence of a functional *Krt17* gene, corresponding to a chronic model for tumor initiation (n=3 biological replicates). For all mice, we acquired tissue sections, RNA, and protein extracts from ear, back, tail, and liver tissues.

Preliminary findings indicate that DNA damage occurs in the HPV16-transgenic model, independent of K17 status. Additionally, this body of work sheds new light on the extent of DNA damage in different epidermal tissue sites in the HPV16-transgenic model. Intriguingly, a pilot study of DMBA-initiated DNA damage reveals a potential induction of K17, a finding that would be congruous with the established inducible nature of K17.

Thesis Committee: Dr. Pierre Coulombe and Dr. Phil Jordan

ACKNOWLEDGEMENTS

Firstly, I would like to express my sincere gratitude to Dr. Pierre Coulombe for his guidance and support during the completion of this thesis. It was an absolute pleasure to be part of such a dynamic laboratory and your generosity of both time and knowledge was very much appreciated. I would also like to thank my secondary reader, Dr. Phil Jordan, for his time and effort in evaluating this thesis. I particularly appreciated your astute feedback after my departmental retreat presentation and your continued advice the past few months.

To Dr. Ryan Hobbs, your mentorship over the past year made the ScM program all the more valuable. I cannot thank you enough for the opportunity to work with you and learn from you. You have taught me how to tackle scientific problems with enthusiasm and rigor.

To Dr. Beau Su, I thoroughly enjoyed working with you on the *in vivo* silencing project when I first got to lab. Additionally, your help with various experiments and support and patience in navigating the lab when I first arrived was very generous of you.

To Fengrong Wang, I am grateful for your insightful critique of this manuscript and your willingness to always help with the troubleshooting of experiments and analysis of data.

To all members of the Coulombe laboratory, I enjoyed working with you over the past year and want to thank you for making the lab such a productive and fun environment. I wish you all the best in your future endeavors. I am also grateful for all the support from the entire Biochemistry and Molecular Biology Department, in particular Dr. Janice Evans and Shannon Gaston who have been tremendously helpful over the past two years.

Thank you to my family: my mum, Margaret, my dad, John, and my brothers, Dominic, Patrick and Olly. Your encouragement, patience and support of my ambitious endeavors and goals has been wonderful.

TABLE OF CONTENTS

Abstract ii

Acknowledgements iii

List of Figures vi

List of Tables viii

List of Abbreviations ix

Introduction 1

Types of intermediate filaments 1

Keratin family of proteins 2

Functional roles of keratins 5

Physiological roles ascribed to Keratin 17 in normal skin epithelia 6

Keratin 17: A role in carcinogenesis 7

Mouse skin carcinogenesis is a multistage process 12

HPV16$^{Tg/+}$ model 14

Two-step chemical carcinogenesis model 15

DNA damage as an indicator of initiation 16

Results 19

Elevated DNA damage in the HPV16$^{Tg/+}$ model compared to wild-type does not appear to be K17 dependent 19

γH2AX-positive cells are exclusively found in the epidermis and there is no apparent dependence on K17 status 23

A tissue specific gradient is established in both male and female mice for the HPV16$^{Tg/+}$ model 28

Quantitative RT-PCR reveals variable expression of DNA damage response elements independent of K17 status 33

K17 appears to be induced upon treatment with the mutagen, DMBA, compared to control 36

Discussion **38**

Materials and Methods **48**

References **54**

Appendix **67**

CV **68**

LIST OF FIGURES

Figure 1.	**Subtypes of intermediate filament proteins**	**2**
Figure 2.	**Introduction to the organization and assembly of keratin proteins**	**4**
Figure 3.	**Genetic ablation of K17 delays tumor onset in a model of basal cell carcinoma**	**10**
Figure 4.	**Loss of K17 attenuates squamous cell carcinoma-like growth**	**12**
Figure 5.	**Multistage model of mouse skin carcinogenesis**	**13**
Figure 6.	**HPV16$^{Tg/+}$ model for squamous cell carcinoma**	**15**
Figure 7.	**γH2AX is a reliable marker of DNA damage**	**17**
Figure 8.	**Elevated DNA damage is exhibited in the HPV16$^{Tg/+}$ setting compared to wild-type in female mice**	**21**
Figure 9.	**Elevated DNA damage is exhibited in the HPV16$^{Tg/+}$ setting compared to wild-type in male mice**	**22**
Figure 10.	**γH2AX levels in HPV16$^{Tg/+}$ mice vs wild-type; male biological replicate 1**	**25**
Figure 11.	**γH2AX levels in HPV16$^{Tg/+}$ mice vs wild-type; male biological replicate 2**	**26**
Figure 12.	**γH2AX levels in HPV16$^{Tg/+}$ mice vs wild-type; male biological replicate 3**	**27**
Figure 13.	**Tissue discordance in γH2AX levels in female mice**	**30**
Figure 14.	**Tissue discordance in γH2AX levels in male mice**	**31**

Figure 15. **Tissue discordance in γH2AX levels in both male and female mice** **32**

Figure 16. **qRT-PCR analyses of DNA damage response-associated gene expression changes** **35**

Figure 17. **K17 may be induced upon systemic treatment with the mutagen, DMBA** **36**

LIST OF TABLES

Materials and Methods

Table 1. **Table of forward and reverse primer sequences used in qRT-PCR analyses of ear, back and tail tissue** **53**

Appendix

Table 2. **Description of qRT-PCR gene targets and the roles of the encoded proteins** **67**

LIST OF ABBREVIATIONS

A431	Human epidermoid carcinoma cell line
AIRE	Autoimmune regulator
Atm:ATM	Ataxia telangiectasia mutated (gene:protein)
Atr:ATR	Ataxia telangiectasia and Rad3-related (gene:protein)
BCC	Basal cell carcinoma
BRCA1	Breast cancer susceptibility gene 1 protein
Chk1:CHK1	Checkpoint kinase 1 (gene:protein)
Chk2:CHK2	Checkpoint kinase 2 (gene:protein)
CRISPR/Cas9	Clustered regularly interspaced short palindromic repeats/CRISPR associated protein 9
DAPI	4',6-diamidino-2-phenylindole
DDR	DNA damage response
DMBA	7,12-Dimethylbenz(a)anthracene
DSB	Double-strand break
E2F	E2 transcription factor
E6	Early gene 6
E7	Early gene 7
EBS	Epidermolysis bullosa simplex
ECL	Enhanced chemiluminescence
ECM	Extracellular matrix
Foxm1	Forkhead box protein M1 gene
GAPDH	Glyceraldehyde 3-phosphate dehydrogenase
Gli2	GLI family zinc finger 2
HaCaT	Human immortalized keratinocyte cell line
H-Ras	Harvey rat sarcoma viral oncogene

hnRNP K	heterogeneous nuclear ribonucleoprotein K
HPV	Human papillomavirus
IF	Intermediate filament
IFN-γ	Interferon gamma
IgG	Immunoglobulin G
IP	Intraperitoneal
IR	Ionizing radiation
K	Keratin protein
kDa	Kilodalton
Krt	Keratin gene
Ku80(XRCC5)	X-ray repair cross-complementing protein 5
MPO	Myeloperoxidase
MW	Molecular weight
nm	Nanometer
OCT	Optimal cutting temperature compound
P50, P120 etc.	Postnatal day 50, 120 etc.
P53	Tumor protein p53
PC	Pachyonychia congenita
PIK	Phosphoinositide 3-kinase
pKa	Acid dissociation constant
qRT-PCR	Real-time quantitative reverse transcription polymerase chain reaction
SCC	Squamous cell carcinoma
SDS-PAGE	Sodium dodecyl sulfate polyacrylamide gel electrophoresis
Shh	Sonic hedgehog
shRNA	Short hairpin RNA
Th1	Type 1 T helper cell
Th17	Type 17 T helper cell

Th2	Type 2 T helper cell
TNF-α	Tumor necrosis factor alpha
TPA	12-O-Tetradecanoylphorbol-13-acetate
TRADD	Tumor necrosis factor receptor type 1-associated death domain protein
UV	Ultraviolet
v/v	Volume/volume
w/v	Weight/volume
WT	Wild-type
Xrcc5	X-ray repair complementing defective repair in Chinese hamster cells 5
γH2AX	Phosphorylated histone variant H2AX
μg	Microgram
μl	Microliter

INTRODUCTION

Types of intermediate filaments

The very basis of cellular architecture, and more specifically the unique structure that various cells retain, is derived from a complex network of fibrous proteins that provide mechanical and structural support, among other roles. These functions are attributed to three kinds of filamentous cytoskeletal proteins, namely microfilaments (F-actin ~6 nm), microtubules (tubulin ~25 nm) and intermediate filaments (IF), defined by their intermediary diameter of ~10 nm (Fuchs and Weber, 1994; Wickstead and Gull, 2011). In part, biochemical analyses and immunofluorescence microscopy have revealed unique subsets of intermediate filaments that could be organized based upon the cell type and subcellular localization (Franke *et al.*, 1978). This was somewhat surprising given the conserved tripartite structure and rod domain sequence largely similar among IF proteins. However, it was ascertained that the variability specific to the amino-terminal and carboxyl-terminal end domains gives rise to the functional diversity of intermediate filaments (Steinert and Roop, 1988). Now, it is understood that intermediate filaments fall into six primary categories with a diverse set of functions, including type V lamins, comprising nuclear lamina, and desmin, a type III IF that plays an integral role in the contractile constituents of myogenic cells (Figure 1; Chung *et al.*, 2013; Paulin and Li, 2004). Due to our concentration on skin biology in the Coulombe laboratory, of particular interest to us are keratin (K) proteins, the type I and type II intermediate filaments, and consequently these IFs will be the focus of the remainder of this thesis.

Subgrouping	Proteins	Cell type specificity
Type I Type II	Keratins	Soft complex epithelia (skin, oral mucosa, etc.) Soft simple epithelia (liver, gut, kidney, etc.) Hard epithelia (hair, nail, oral papillae)
Type III	Vimentin, Desmin GFAP, Peripherin syncoilin	Various (fibroblasts, leukocytes, endothelium muscle, astrocytes, glia, peripheral nerves)
Type IV	NF-L, NF-M, NF-H a-internexin synemin, nestin	CNS & neurons CNS & neurons Muscle, neural stem cells
Type V	Lamins A, B & C	Nucleus
Orphan	Filensin, Phakinin	Lens

Figure 1. Subtypes of intermediate filament proteins
Intermediate filaments are predominantly organized into six different groups based on their tissue specificity and subcellular localization. Keratin proteins are found in the Type I and Type II groups. From Chung et al., 2013.

Keratin family of proteins

Keratins are i) the largest family of intermediate filaments (with 54 genes in total), ii) characteristically epithelial in origin and iii) have molecular weights (MW) ranging from 40 to 70 kDa (Schweizer *et al.*, 2006; Sun *et al.*, 1983). They are classified as type I or type II based on several molecular features, including gene substructure and sequence homology (Figure 2A; Fuchs and Marchuk, 1983). In particular, type I keratins are acidic (pKa 4.5-5.5) whereas type II keratins are neutral or basic (pKa 6.5-8.5) (Fraser *et al.*, 1972; Moll *et al.*, 1982). Moreover, keratins have a number of key features including, but not limited to, the distinctive ability to self-assemble *in vitro* (Figure 2B) and to remain cytoplasmic under normal physiological conditions (Figure 2C) (Coulombe and Omary, 2002; Yamada *et al.*, 2002).

As previously mentioned, keratins have a tripartite structure with a N-terminal head, central rod and C-terminal tail domains. Additionally, the central rod domain is comprised of α-helical subdomains of fixed length (1A, 1B, 2 A, 2B) separated by short linker regions (Figure 2D; Bragulla and Homberger, 2009). The central rod domain of keratins features long-range

heptad repeat of hydrophobic/apolar amino acids that permit a unique coiled-coil interaction which preferentially forms between a type I and type II partner (Coulombe and Fuchs, 1990; Hatzfeld and Weber, 1990). Subsequent interactions between heterodimers lead to the formation of anti-parallel tetramers and ultimately to a ~10 nm wide keratin filament composed of lateral and longitudinal aggregations of these elongated tetrameric and octameric subunits (Aebi *et al.*, 1983).

Reflecting in part a strict requirement for the heteromeric assembly of their protein products, type I and type II keratin genes are regulated in a pairwise, tissue- and differentiation-specific fashion in epithelial cells. For example, the type II *Krt5* and type I *Krt14* genes are co-expressed in the basal progenitor layer of epidermis and related complex epithelia, whereas the type II *Krt8* and type I *Krt18* genes are expressed in simple epithelia such as gut, liver, kidney and others (Coulombe and Fuchs, 1990; Schutte *et al.*, 2004).

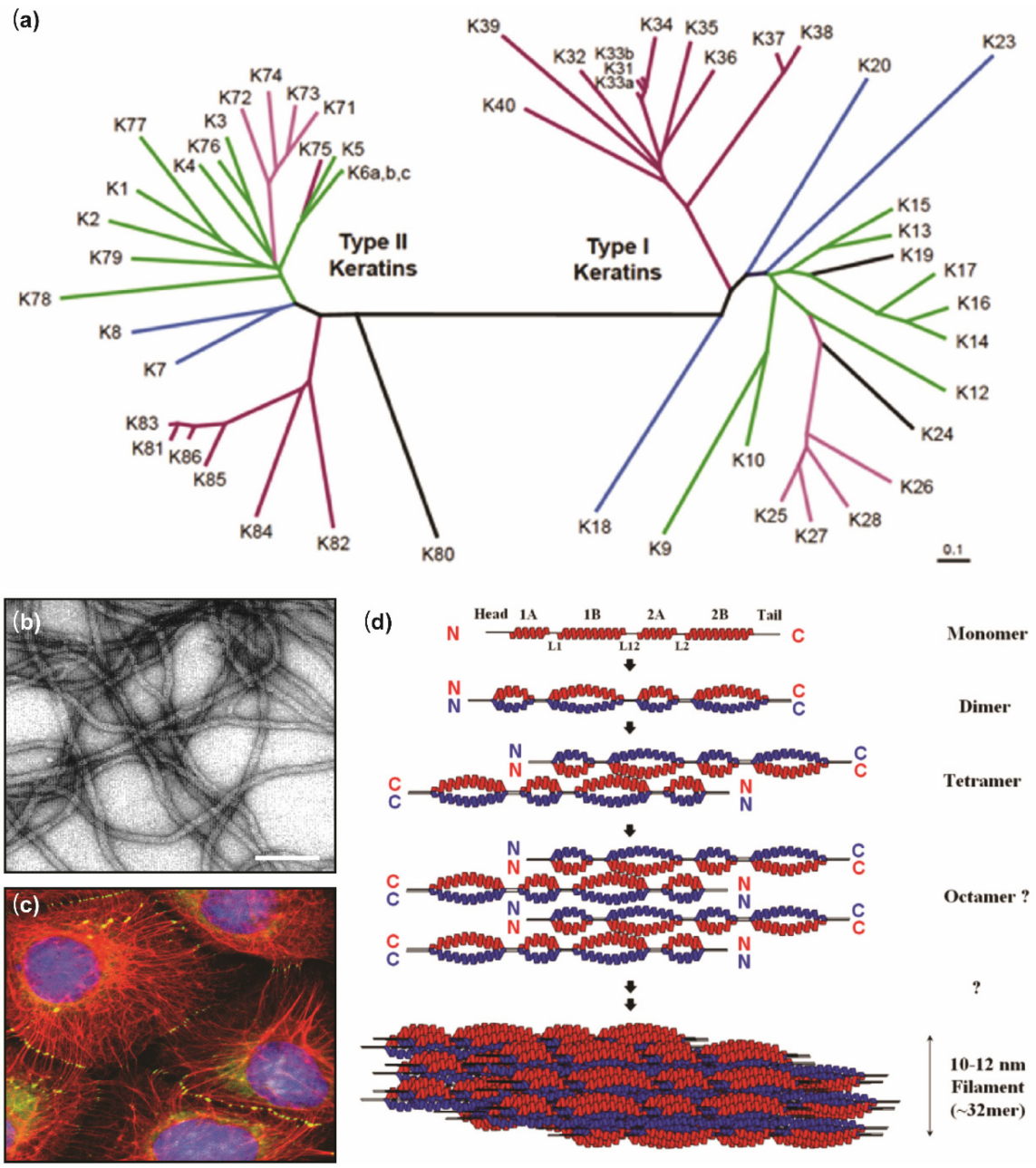

Figure 2. Introduction to the organization and assembly of keratin proteins.
(a) The 54 keratin proteins are organized into type I ("acidic") and type II ("basic to neutral") groupings that pair to form heteropolymeric filaments. (b) Electron microscopy image of IFs reconstituted in vitro from purified human K5 and K14 proteins. Scale bar, 100 μm. (c) Immunofluorescent staining of cytoplasmic localization of keratin filaments. Blue staining is DAPI. (d) Schematic demonstrating the assembly of keratin proteins into 10-12 nm filaments. The heterodimerization of type I and type II keratins occurs in a parallel and polar fashion. However, the formation of a tetramer proceeds in an apolar manner. Figure adapted from Coulombe et al., 2012.

Functional roles of keratins

The notion that intermediate filaments, and keratins in particular, merely play structural roles has undergone a momentous paradigm shift. Although type I and II keratins are absolutely essential in maintaining cellular architecture, supporting the nucleus and providing mechanical resilience to a cell, a number of ancillary functions have been uncovered that underscore the pleiotropic nature of these proteins (Kim and Coulombe, 2007; Pallari and Eriksson, 2006; Toivola *et al.*, 2010). In this section, both the mechanical and non-mechanical capacities of keratin proteins will be briefly discussed.

A variety of external and internal stimuli can impose substantial stress upon cells, most notably in the skin. In response, eukaryotic epithelial cells have adapted means of withstanding the impact of mechanical forces through intricate networks of cytoplasmic keratin filaments. The micromechanical properties of keratins become most apparent in disease settings where mutations in keratin genes causes a variety of skin-related aberrations (Gu and Coulombe, 2007). For example, two genetic diseases, epidermolysis bullosa simplex (EBS) and pachyonychia congenita (PC), are characterized by skin fragility and disrupted tissue architecture and homeostasis respectively, underscoring the structural role that keratins play (Coulombe and Fuchs, 1993; McLean *et al.*, 1995).

Furthermore, keratins interact with organelles through a number of mechanisms. They have been implicated in having a functional relationship with mitochondria and in the cellular distribution of Golgi apparatus, evident in the dysregulation of Golgi reassembly in a cell line expressing a mutated K18 protein (Toivola *et al.*, 2005). Keratins also have a capacity to target cellular proteins and are implicated in a variety of cellular signaling processes, readily apparent for the type I protein, keratin 17 (K17).

Physiological roles ascribed to K17 in normal skin epithelia

At baseline, K17 has a complex expression pattern. It is constitutively expressed in the hair follicle and other ectoderm-derived epithelial appendages (nail, glands, tooth, and thymus) and is displayed only in cells of certain types of complex epithelia (McGowan and Coulombe, 1998; Panteleyev *et al.*, 1997; Troyanovsky *et al.*, 1989). Much of our knowledge about K17 in normal physiology has extended from initial observations in a K17 null mouse model (McGowan and Coulombe, 2002). As would be expected, K17, although absent from the interfollicular epidermis, plays a structural role in the postnatal hair follicle. This manifests itself in two primary functions: 1) providing mechanical strength and resistance to the hair shaft and 2) maintaining the viability of hair-producing epithelial cells in the outer root sheath and matrix (McGowan and Coulombe, 2002).

Consistent with the findings by Oshima (2002) that keratins influence apoptotic signaling, additional studies on K17 in the hair follicle have revealed a specific relationship between K17 and TNF-α in regulating normal hair follicle cycling (Tong and Coulombe, 2006). TNF-α is an endogenous pyrogen with a broad array of physiological responsibilities including inducing inflammation and apoptotic cell death. The molecular interaction between K17 and the TNF-α adaptor protein, TRADD, is required for the proper anagen-catagen transition (transition from the growth phase to the involution phase of the hair cycle), which would be otherwise disrupted by TNF-α (Commo and Bernard, 1997; Tong and Coulombe, 2006). This provides a concrete function for K17 in epithelial signaling pathways that extends beyond the established canonical roles for IFs.

A study by Kim *et al.* (2006) uncovered a newfound function of K17 in the Akt/mTOR signaling pathway and regulation of cell growth through the direct binding with the accessory protein 14-3-3*σ*. This is particularly notable in the context of tissue and wound repair. Using

cell mass and size as readouts, K17 knockout primary keratinocytes were significantly reduced in size as a result of attenuated *de novo* protein synthesis and, additionally, $K17^{-/-}$ embryos exhibited subsequent altered wound closure *in vivo* (Kim *et al.*, 2006). This novel finding was striking and, as such, verification of this as a K17-specific role was necessary. Indeed, further biochemical analyses validated these findings and honed in on two particular amino acid residues in the amino-terminal head domain (Ser 9 and Ser 44) that are indispensable for these functions (Kim *et al.*, 2006). Additionally, extensive studies on K17 in both disease settings and developmental processes of the skin have revealed its inducible nature (McGowan and Coulombe, 1998), hinting at potentially unrecognized contributions of K17.

Keratin 17: A role in carcinogenesis

The body of evidence that Keratin 17, a 46 kDa type I keratin, plays a functional role in carcinogenesis has been mounting. Preliminary research on a '46,000 molecular weight (MW) cytokeratin', now recognized as K17, corroborated its apparent absence from interfollicular epithelial tissue and uncovered its distinctive prominence in basal cell epithelioma (BCC) (Moll *et al.*, 1982). Capitalizing on the generation of highly specific monoclonal antibodies for immunohistochemistry, Markey *et al.* (1992) confirmed in a study of 15 human patient samples the BCC-derived K17 expression *in situ*. Although these discoveries were momentous from a basic physiology standpoint, the true significance of K17 in carcinogenesis was demonstrated through a comprehensive microarray of breast cancer tissue samples (van de Rijn *et al.*, 2002). Herein, the authors analyzed over 600 paraffin-embedded breast tumors and found a compelling association between the expression of K17 in breast carcinoma cells and a poorer prognosis, as demonstrated by Kaplan-Meier survival analysis.

Investigation of K17 in other pathologies has provided a more detailed insight into the molecular mechanisms by which K17 contributes to cancer. Early studies on psoriasis indicated that treatment with anti-psoriatic therapy dramatically reduced K17 expression in suprabasal keratinocytes (de Jong *et al.*, 1991). This observation was striking as K17 had not been observed in healthy epidermal tissue but was upregulated in psoriatic conditions. *In vitro* studies in the human keratinocyte cell line, HaCaT, provided a mechanistic context in which K17 was involved in psoriatic lesions. In particular, IFN-γ, a central cytokine in the pathogenesis of psoriasis, was shown to transcriptionally activate K17 and the overexpression of IFN-γ led to hyperproliferation and dysregulated differentiation of keratinocytes (Bonnekoh *et al.*, 1995; Vogel *et al.*, 1995). These examples are not exhaustive since K17 induction has been reported in a variety of other stress-related settings such as viral infection, acne and injury, to name a few (Hughes *et al.*, 1996; Jin and Wang, 2013; Pan *et al.*, 2011; Proby *et al.*, 1993).

The common feature of many of these conditions is a robust inflammatory response, prompting the question whether K17 has a functional role in other settings with a similar context. As such, and building on the work conducted by van de Rijn *et al.* (2002) in breast cancer, K17 has now been identified as a prognostic marker and/or indicator of poorer clinical outcomes in a variety of epithelial-derived cancers including, cervical, ovarian, oral squamous cell carcinomas and gastric adenocarcinoma (Escobar-Hoyos *et al.*, 2014; Ide *et al.*, 2012; Kitamura *et al.*, 2012; Wang *et al.*, 2013). Unifying these two observations is the well-established connection between inflammation and cancer (Coussens and Werb, 2002; Lin and Karin, 2007). Accordingly, significant efforts have been undertaken in the Coulombe laboratory to delineate the relationship between K17, inflammation and cancer in the skin.

The advent of transgenic mouse models has opened up new avenues through which to enhance our understanding of cancer pathophysiology. A transgenic model for basal cell carcinoma (BCC) has been pivotal for developing a deeper understanding of how K17 is involved in carcinogenesis. The K5 promoter-driven overexpression of the transcription factor Gli2 results in the activation of the Sonic hedgehog (Shh) signaling pathway in an oncogenic manner. In turn, this leads to the development of multiple BCC lesions on ear, tail and trunk tissue (Grachtchouk *et al.*, 2000). However, the genetic ablation of *Krt17* in this setting impairs BCC lesion development and dramatically reduces the extent of epidermal hyperplasia (Figure 3A; DePianto *et al.*, 2010). In both male and female mice, there is a significant delay in lesion onset as a result of K17 ablation (Figure 3B and 3C; DePianto *et al.*, 2010). Underpinning this is a reduction in inflammation and diminished level of cell proliferation that was seen in the Gli2^{tg}; *Krt17*$^{-/-}$ mice, as revealed by a 3-fold reduction in mitotically active cells (DePianto *et al.*, 2010). qRT-PCR analyses have also exhibited a global shift in cytokine expression, from Th1/Th17 ('pro-inflammatory') to Th2 ('anti-inflammatory'), further complementing these findings (DePianto *et al.*, 2010).

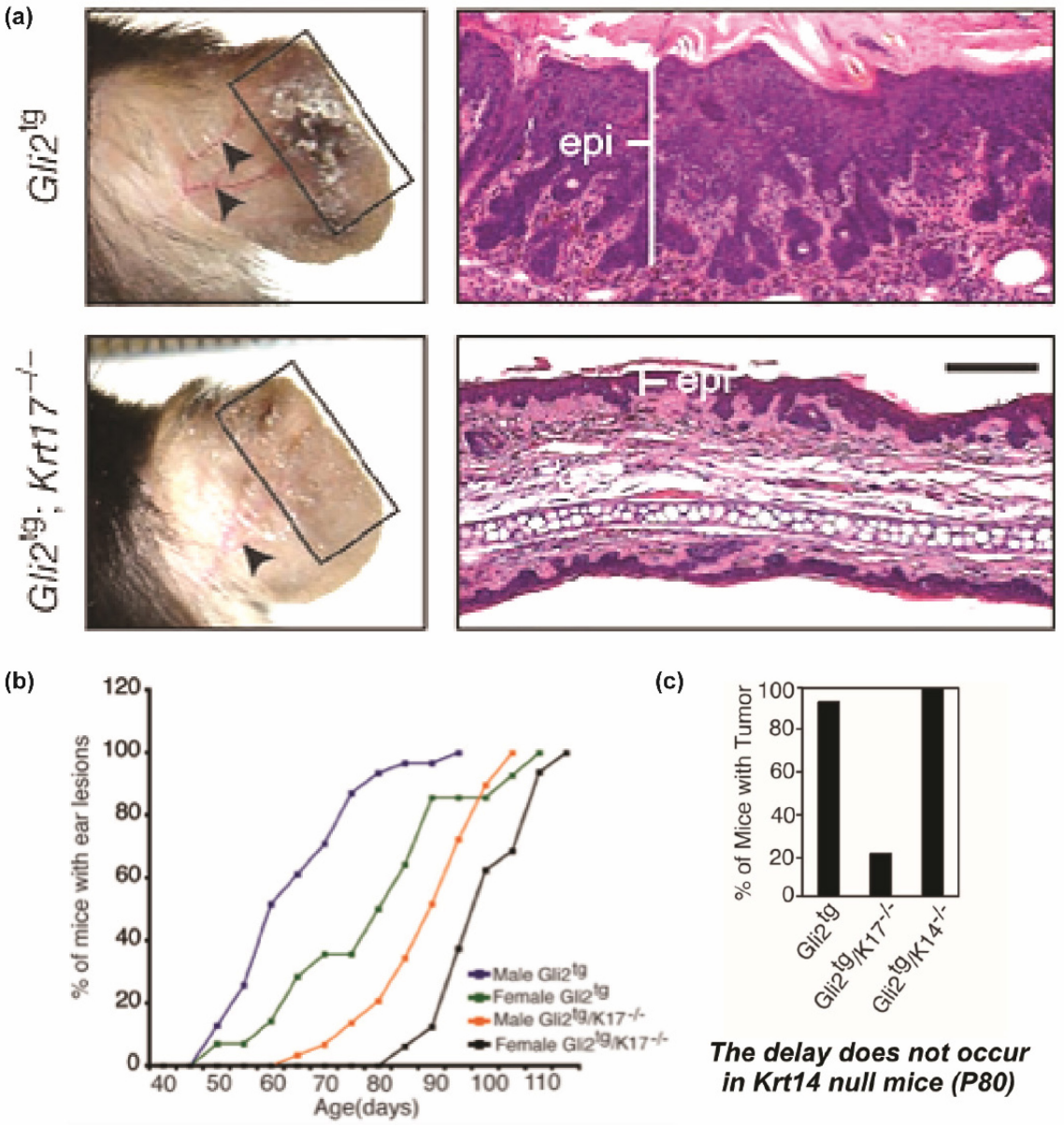

Figure 3. Genetic ablation of K17 delays tumor onset in a model of basal cell carcinoma. (a) Left panel indicates that P80 Gli2^{Tg} mice spontaneously develop ear lesions however in K17 null mice the onset of these BCC-like lesions is delayed. Right panel, hematoxylin-eosin stained ear tissue demonstrating a dramatic reduction in the thickness of the ear epithelium upon genetic ablation of K17. (b) Cumulative percentage of mice with ear lesions stratified by sex and genotype during P40-P120 time frame. Both males and females exhibit delayed tumor onset and no significant difference in the length of the delay is evident between sexes. (c) Quantification of delay in K17 mice at P80 and representative of this as a K17-specific effect when compared with K14 null mice. Figure adapted from DePianto et al., 2010.

Building upon this work, a separate transgenic mouse model for squamous cell carcinoma (SCC) developed by Arbeit *et al.* (1994) was utilized to substantiate the impact of K17 on tumorigenesis. The human papillomavirus (HPV) is widely associated with a plethora of cancers and the targeted expression of HPV type 16 (HPV16) early genes in basal keratinocytes leads to SCC-like lesion formation in the skin, discussed in detail in the next section (Arbeit *et al.*, 1994; Munoz *et al.*, 2006). Correspondingly, genetic ablation of K17 in the HPV16$^{Tg/+}$ setting (HPV16$^{Tg/+}$; *Krt17*$^{-/-}$) markedly reduces epidermal thickness in ear tissue, concomitant with alterations in determinants of tumor growth: angiogenesis, inflammation and mitotic activity (Figure 2A; Hobbs *et al.*, 2015). To dissect the mechanism by which K17 regulates pro-inflammatory gene signatures, a number of *in vitro* assays pointed to an interaction between K17, autoimmune regulator (Aire) and the ribonucleoprotein, hnRNP K, in impacting cytokine production (Figure 2B; Chung *et al.*, 2015; Hobbs *et al.*, 2015).

Epidermal malignancies are not the only setting in which K17 has a culpable role in carcinogenesis. Using the same HPV16$^{Tg/+}$ model, Hobbs *et al.* (2015) showed that loss of K17 attenuates disease progression in cervical cancer and has a more complex function than initially postulated, as the effects of K17 loss on immune response and inflammatory gene expression were distinct in this setting. This is further coupled with the findings that K17 influences cell adhesion and oncogenic transformation in the relatively uncommon bone cancer, Ewing sarcoma (Sankar *et al.*, 2013). Although K17 plays an intricate part in inflammatory processes that directly influence tumor development, it is evident that these tissue-specific nuances encourage further investigation of a potentially more expansive role for K17 in cancer (Hobbs. *et al., 2015;* Sankar *et al.*, 2013).

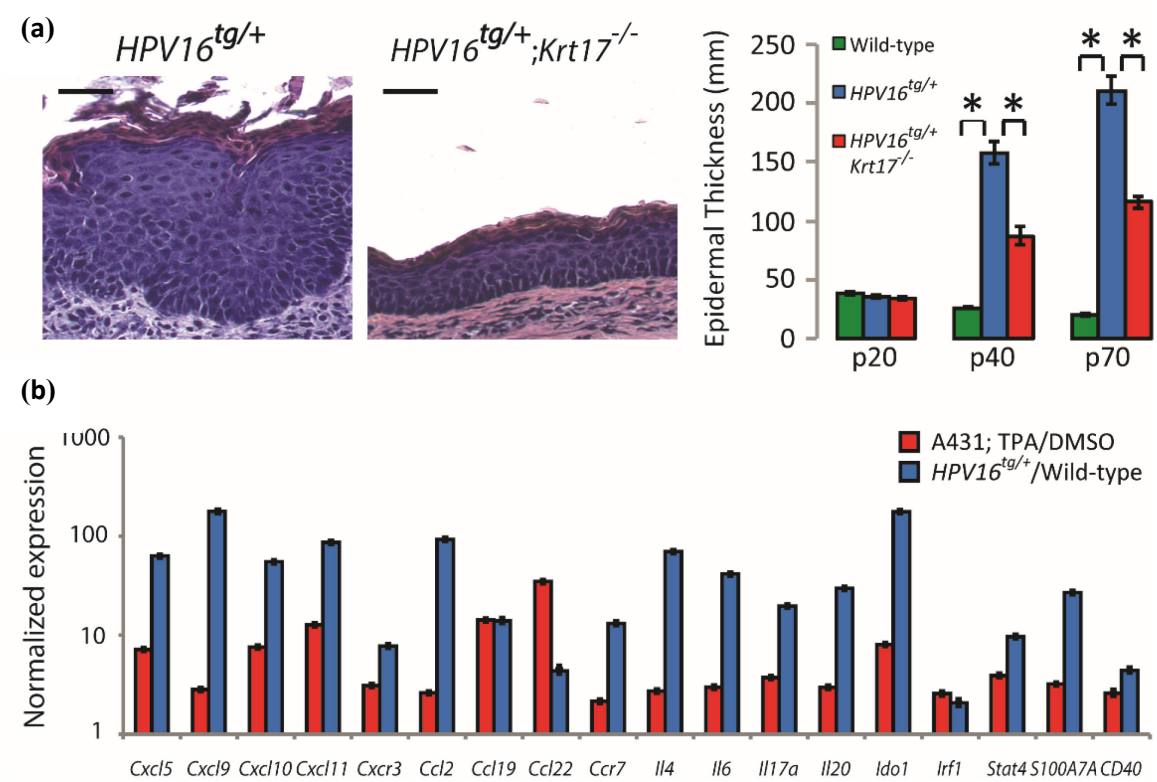

Figure 4. Loss of K17 attenuates squamous cell carcinoma-like growth.
(a) Hematoxylin-eosin stain of HPV16$^{Tg/+}$ and HPV16$^{Tg/+}$; *Krt17*$^{-/-}$ mouse ear sections at P70 demonstrating a substantial increase in epidermal thickness. Quantification of epidermal thickness at both pre-lesional and lesional time points across wild-type, HPV16$^{Tg/+}$ and HPV16$^{Tg/+}$; *Krt17*$^{-/-}$ genotypes. Scale bars, 20 μm. Error bars, s.e.m. (b) *In vitro* analyses indicate that K17 induces a pro-inflammatory response based on the normalized expression levels of the 19 genes represented above. Figure adapted from Hobbs et al., 2015.

Mouse skin carcinogenesis is a multistage process

Mouse skin provides a favorable stage for a more detailed investigation of the mechanisms that drive tumorigenesis for a number of reasons. Firstly, murine skin is readily accessible for tissue and sample procurement, macroscopic evaluation of lesions as they progressively develop, and treatment interventions. Secondly, the architecture of stratified squamous epithelium is well understood and a number of transgenic mouse models for skin cancer have been established (i.e. Gli2^{tg} and HPV16$^{Tg/+}$), enabling efficient genetic manipulation of the molecular target of interest. Lastly, mouse skin tumor development is

step-wise and ordered into discrete initiation, promotion and progression stages (Figure 5; Slaga *et al.*, 1996). Broadly speaking, inflammation is a characteristic of each of these stages and, to date, the role of K17 in explicit stages of tumorigenesis has yet to be established. The models described, herein, will enable the identification of the stage(s) at which K17 may be playing a role during skin epithelial carcinogenesis.

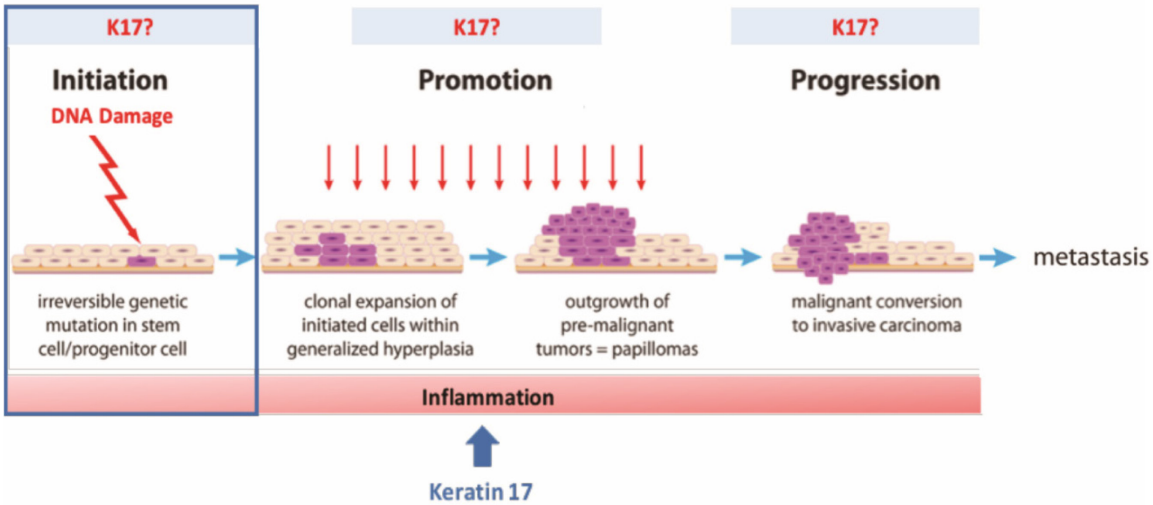

Figure 5. Multistage model of mouse skin carcinogenesis.
An oncogenic event, either chemical or genetic, is the major characteristic of the initiation stage of carcinogenesis. This insult can either be an activating mutation in a proto-oncogene or an inactivating mutation in a tumor suppressor gene. The promotion phase is characterized by a stark increase in pro-inflammatory elements leading to epidermal hyperplasia. Additionally, these oncogenic insults lead to clonal expansion of the mutated cells. Progression results in the conversion of benign papillomas to invasive and malignant carcinomas resulting in widespread outgrowth of cancer cells and subsequent metastasis. Previous studies have demonstrated the involvement of Keratin 17 in the pro-inflammatory response, however no such work has been conducted on the association between K17 and the specific stages of carcinogenesis. Figure adapted from Rundhaug and Fischer, 2010.

In short, the initiation stage of carcinogenesis is characterized by an irreversible oncogenic event leading to DNA damage that occurs in a small number of susceptible skin epithelial cells. The effectors of this damage vary, including UV exposure and chemical carcinogens. However, in similar fashion, they all cause genetic alterations in either tumor suppressor (e.g. *TP53/Trp53*) or proto-oncogenes (e.g. *H-Ras*) that 'initiate' the process of

tumor formation (Hennings *et al.*, 1993; Quintanilla *et al.*, 1986). These few transformed cells then undergo clonal expansion, aided by inflammatory processes, and often distinguished by a selective growth advantage over normal cells (Yuspa *et al.*, 1982). Finally, the progression stage is typified by malignant transformation of cancer cells, as identified by increased genomic instability and telomerase activity, disrupted ECM interactions and metastasis (Bednarek *et al.*, 1995; Tennenbaum *et al.*, 1992).

HPV16$^{Tg/+}$ model

The HPV16$^{Tg/+}$ transgenic mouse is an elegant model for studying the development of HPV-induced SCC. Variability exists in the extent of neoplastic progression according to the specific virus type. Consequently, HPV type 16 was selected on the basis of its ability to cause high-grade lesions (Arbeit *et al.*, 1994). This capacity largely arises from two specific 'early' genes in the HPV genome: E6, which explicitly targets and degrades P53 and E7, which ultimately permits the release of the transcription factor, E2F, leading to increased and improperly regulated cellular proliferation (Figure 6A; Chellappan *et al.*, 1992; Scheffner *et al.*, 1990). By using a K14 promoter to preferentially drive HPV16 transgene expression in basal keratinocytes (which express the K5 and K14 filaments), this model successfully targets the most proliferative cells in the epidermis, as well as the cells that are most affected by SCC lesions. Moreover, the invasive nature of the HPV16 virus results in full insertion into the host genome suggesting that DNA double strand breaks are a particularly common type of DNA damage in this setting (Gillespie *et al.*, 2012; Williams *et al.*, 2014). In this model, lesion onset tends to occur at postnatal day 60 (P60). Thus, the 'prelesional' time point at P50 is most similar to what would be considered the initiation stage (Figure 6C; Hobbs *et al.*, 2015). By P120 there is complete penetrance of macroscopic lesion formation in ear tissue with

hyperkeratosis (Figure 6D). Notably, there is a robust upregulation of K17 between P20 and P40 in the interfollicular epidermis of the HPV16$^{Tg/+}$ model that precedes the time point selected in these studies (Hobbs *et al.*, 2015).

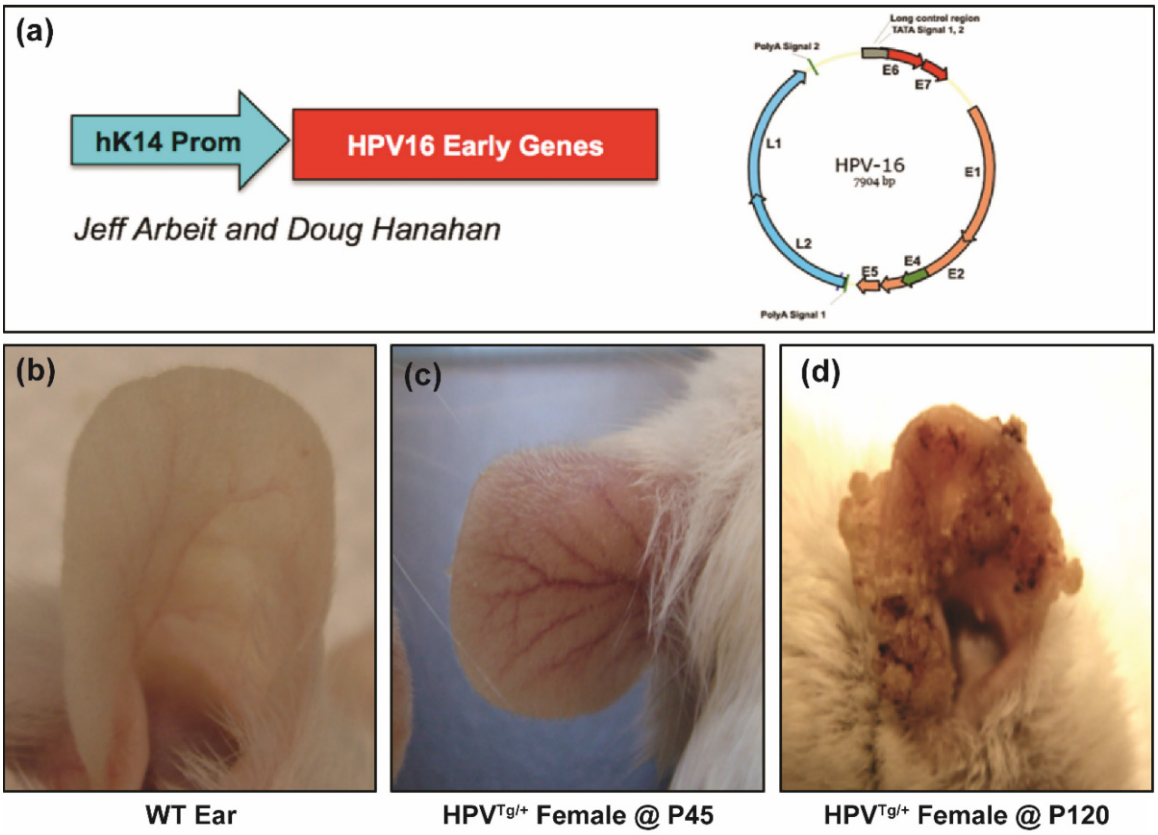

Figure 6. HPV16$^{Tg/+}$ model for squamous cell carcinoma.
(a) Schematic depicting the K14 promoter, a keratin constitutively expressed in basal cells of the epithelium, driving the early genes of the human papillomavirus type 16 (HPV16), in particular E6 and E7, that gives rise to squamous cell carcinoma (SCC). (b) Representative image of a normal, wild-type ear. (c) and (d) depict ears of the HPV16 transgenic mouse model. (c) Image of a pre-lesional HPV16$^{Tg/+}$ female ear at P45 with increased vasculature. (d) Image of HPV16$^{Tg/+}$ ear at P120 with significant squamous cell carcinoma growth. Adapted from Coulombe, 2016; Figure adapted from Doorbar, 2006.

Two-step chemical carcinogenesis model

Pharmacological induction of carcinogenesis in mouse skin provides an additional route to evaluate the various contributions of molecular entities to tumor development. Traditionally, in the two-step chemical carcinogenesis model, two separate agents are used to

chemically elicit the stages of initiation and promotion. 7,12-dimethylbenz[a]anthracene (DMBA) is a polycyclic aromatic hydrocarbon frequently used for its ability to cause widespread DNA damage. Specifically, DMBA administration causes an A to T transversion in the *H-Ras* gene with relatively high frequency, including in keratinocyte stem cells, which are thought to be the primary cellular target during initiation (Brown *et al.*, 1990; Morris, 2004). Other mutagens can also be used to initiate cells in the two-step chemical carcinogenesis model reviewed by Abel *et al.* (2009).

Once initiated with a mutagen such as DMBA, a second exposure is used to enact the promotion stage of carcinogenesis. Again, a variety of agents can induce this phase. However, the most common one is the phorbol ester, 12-*O*-tetradecanoylphorbol-13-acetate (TPA) (Abel *et al.*, 2004). Upon treatment with TPA, there is a robust and enhanced inflammatory response in the skin that spurs the formation of papillomas and subsequent invasive carcinomas (Mueller, 2006). Interestingly, using the A431 epidermoid carcinoma cell line, Hobbs *et al.* (2015) demonstrated that inflammatory cytokine induction by TPA treatment was K17-dependent and that shRNA knockdown or CRISPR/Cas9-mediated knockout of K17 dramatically attenuated this TPA induction of cytokine expression. Of significant value to biological researchers is the fact that the stages of carcinogenesis and chemical administrations in this acute model can be separated both operationally and mechanistically (Abel *et al.*, 2004).

DNA damage as an indicator of initiation

To properly ascertain the involvement of certain proteins (i.e. K17) in the initiation stage of carcinogenesis, a suitable transgenic mouse model or acute two-step treatment paradigm must be combined with an appropriate experimental readout. DNA damage is a

hallmark of initiation, since mutagenic events give rise to the 'initiated' cells primed for clonal expansion, and thus serves these purposes best.

In reaction to this insult, a number of DNA damage response (DDR) pathways are activated and, depending on the type of insult, certain pathways take charge to repair the damaged DNA. Collectively, this network functions through signal transduction cascades to prompt damage sensors, arrest cell cycle progression and recruit repair machinery to ultimately determine the fate of the cell at hand (Zhou and Elledge, 2000). Two central transducers of the DNA damage response are the phospho-inositide kinase (PIK)-related proteins, ATR and ATM (Zhou and Elledge, 2000). In turn, these proteins target the checkpoint kinases, CHK1 and CHK2, respectively (Figure 7). Other noteworthy effectors are P53, colloquially known as 'the guardian of the genome', and BRCA1 (Lane, 1992). Yet, the network of DDR signaling is rather complex and a reliable proxy that broadly signifies the occurrence of DNA damage is necessary.

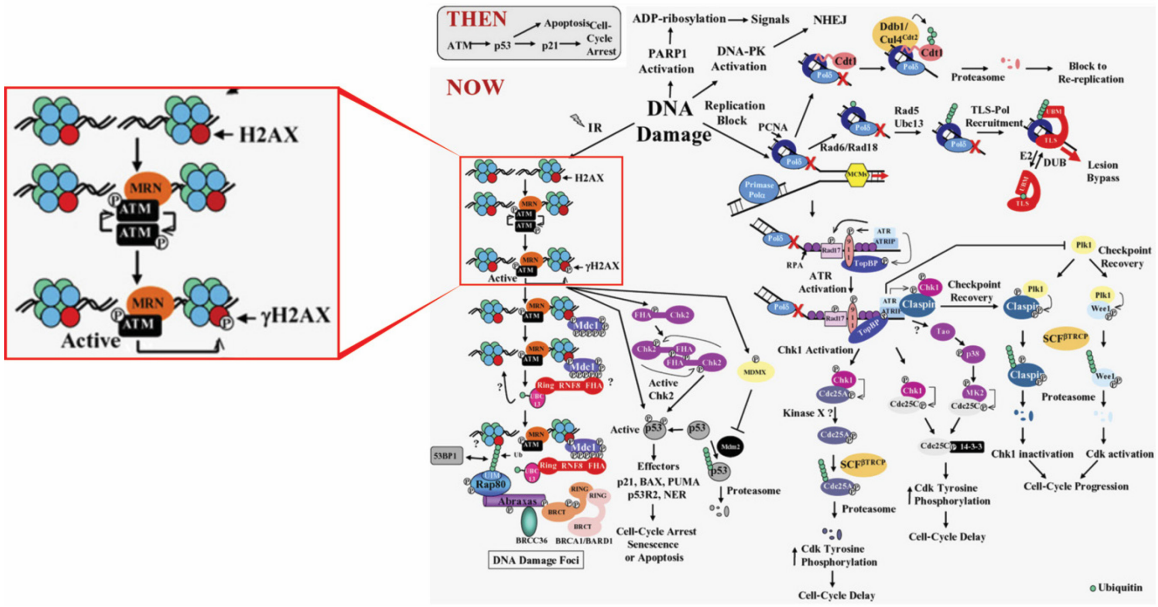

Figure 7. γH2AX is a reliable marker of DNA damage
The DNA damage response (DDR) pathways are a complex network that collectively integrate and respond to a variety of mutagenic insults. The phosphorylation of the histone variant H2AX (to γH2AX) occurs rapidly through ATM-mediated signaling and is an easily detectable and reliable readout for the occurrence of DNA damage. Adapted from Harper and Elledge, 2007.

Phosphorylation of the histone variant H2AX on serine-139 (thereafter referred to as γH2AX) rapidly occurs upon DNA damage, in particular upon double-strand breaks (DSBs) (Figure 7). In fact, the formation of γH2AX foci occurs within seconds of DNA damage, however it is more reliably detected 15-30 minutes after the insult (Sharma *et al.*, 2012). Moreover, the number of foci is directly indicative of the extent of DNA damage as each foci represents a single DSB (Löbrich *et al.*, 2010). This phosphorylation event not only modifies chromatin structure thus enabling repair machinery to more readily access affected DNA, but also acts to recruit DDR-associated proteins.

The reliability of this marker has been widely documented due to its distinct advantages over comparable DDR proteins (BRCA1, 53BP1 etc.), including the fact that it is detectable in all cell cycle phases, as opposed to the more restricted expression of others (Polo and Jackson, 2011). Practically, it has been used in a number of different experimental assays: immunoblotting, immunostaining of tissue sections and flow cytometry, all of which enable the application of efficient quantification methods (Mah *et al.*, 2010; Sharma *et al.*, 2012). Suitably, a number of the experimental assays described in this thesis exploit the reliability and efficiency of this DNA damage marker.

As an additional means of pinpointing the relationship between K17 and DNA damage, qRT-PCR analyses for prominent DDR genes was conducted, including those encoding for the major effectors of these signaling pathways. A detailed description of each target gene can be found in Appendix A.

RESULTS

Elevated DNA damage in the HPV16$^{Tg/+}$ model compared to wild-type does not appear to be K17 dependent

The HPV16$^{Tg/+}$ model is a well-defined and previously reported paradigm for the development of intraepithelial lesions and subsequent squamous cell carcinomas that parallel those seen in human skin (SCC) (Arbeit *et al.*, 1994; Hobbs *et al.*, 2015). Prior documented research indicated that lesion development occurs between P60 and P120 in HPV16$^{Tg}/^{+}$ ear skin, with complete penetrance by P120 (Hobbs *et al.*, 2015). As such, the pre-lesional time point defined for these studies reported here was determined to be P50. This time point coincides with characteristics that are shared by the initiation phase of carcinogenesis, including increased vascularization ("angiogenic switch"), heightened inflammation and cellular proliferation and suppression of apoptotic signaling (Coussens and Werb, 2002; Evan and Vousden, 2001; Hanahan and Folkman, 1996). More significantly, the P50 time point follows the upregulation of K17 in the interfollicular epidermis of HPV16$^{Tg/+}$ mice between P20 and P40 (Hobbs *et al.*, 2015). Further, the analyses reported below were conducted for both male and female mice, based on our previous findings of a sex bias in Gli2-induced tumorigenesis in mouse skin as well as in the hypertrophic and inflamed palmoplantar keratoderma lesions that spontaneously arise in K16 null mice (DePianto *et al.*, 2010; Kerns *et al.*, 2016; unpublished data from the Coulombe laboratory).

To answer the question whether K17 plays a role in DNA damage processes prior to lesion onset in the HPV16$^{Tg/+}$ model, tissue sections from pre-lesional male and female mice were obtained for the WT; *Krt17*$^{+/-}$, HPV16$^{Tg/+}$; *Krt17*$^{+/-}$ and HPV16$^{Tg/+}$; *Krt17*$^{-/-}$ genotypes

and analyzed for DNA damage markers. At the protein level, elevated DNA damage, demonstrated by immunoblotting for the histone variant γH2AX, is evident at the P50 time point in the HPV16$^{Tg/+}$ female mice with or without a functional K17 gene (Figure 8). Indeed, there is a statistically significant increase in γH2AX in HPV16$^{Tg/+}$; *Krt17*$^{+/-}$ and HPV16$^{Tg/+}$; *Krt17*$^{-/-}$ back tissue compared to wild-type (p=0.01 and p=0.0001 respectively). The presence of K17 does not appear to significantly affect the amount of DNA damage present at that time point, in this model (p=0.78). A similar trend was apparent in the ear samples of both transgenic mouse cohorts compared to their wild-type counterparts (HPV16$^{Tg/+}$; *Krt17*$^{+/-}$ vs WT, p=0.01; HPV16$^{Tg/+}$; *Krt17*$^{-/-}$ vs WT, p=0.047, HPV16$^{Tg/+}$; *Krt17*$^{+/-}$ vs HPV16$^{Tg/+}$; *Krt17*$^{-/-}$, p=0.06). By contrast, tail tissue of all mice analyzed in this study did not exhibit pronounced levels of γH2AX, regardless of the genotype (Figure 8, 9).

Correspondingly, male mice examined across all tissue sites and genotypes, exhibited an analogous phenomenon. Back tissue harvested from transgenic mice had elevated γH2AX protein levels compared to wild-type (HPV16$^{Tg/+}$; *Krt17*$^{+/-}$ vs WT, p=0.028; HPV16$^{Tg/+}$; *Krt17*$^{-/-}$ vs WT, p=0.041), despite the lack of a significant difference between HPV16$^{Tg/+}$; *Krt17*$^{-/-}$ and HPV16$^{Tg/+}$; *Krt17*$^{+/-}$ mice (p=0.84). Ear tissue isolates in the male HPV16$^{Tg/+}$ setting displayed increased γH2AX compared to wild-type (HPV16$^{Tg/+}$; *Krt17*$^{+/-}$ vs WT, p=0.045; HPV16$^{Tg/+}$; *Krt17*$^{-/-}$ vs WT, p=0.05) and no disparity arose between K17 heterozygous and null mice in the HPV16$^{Tg/+}$ setting (p=0.70). The tail tissue lacked a noticeable amount of γH2AX. Consistent with previously published research by Hobbs *et al.* (2015), Keratin 17 protein levels displayed a greater than 2-fold increase in the HPV16$^{Tg/+}$ setting compared to wild-type at P50 (note that the substantive K17 levels detected in normal skin tissue at baseline reflect its expression in epithelial appendages, mostly hair follicles).

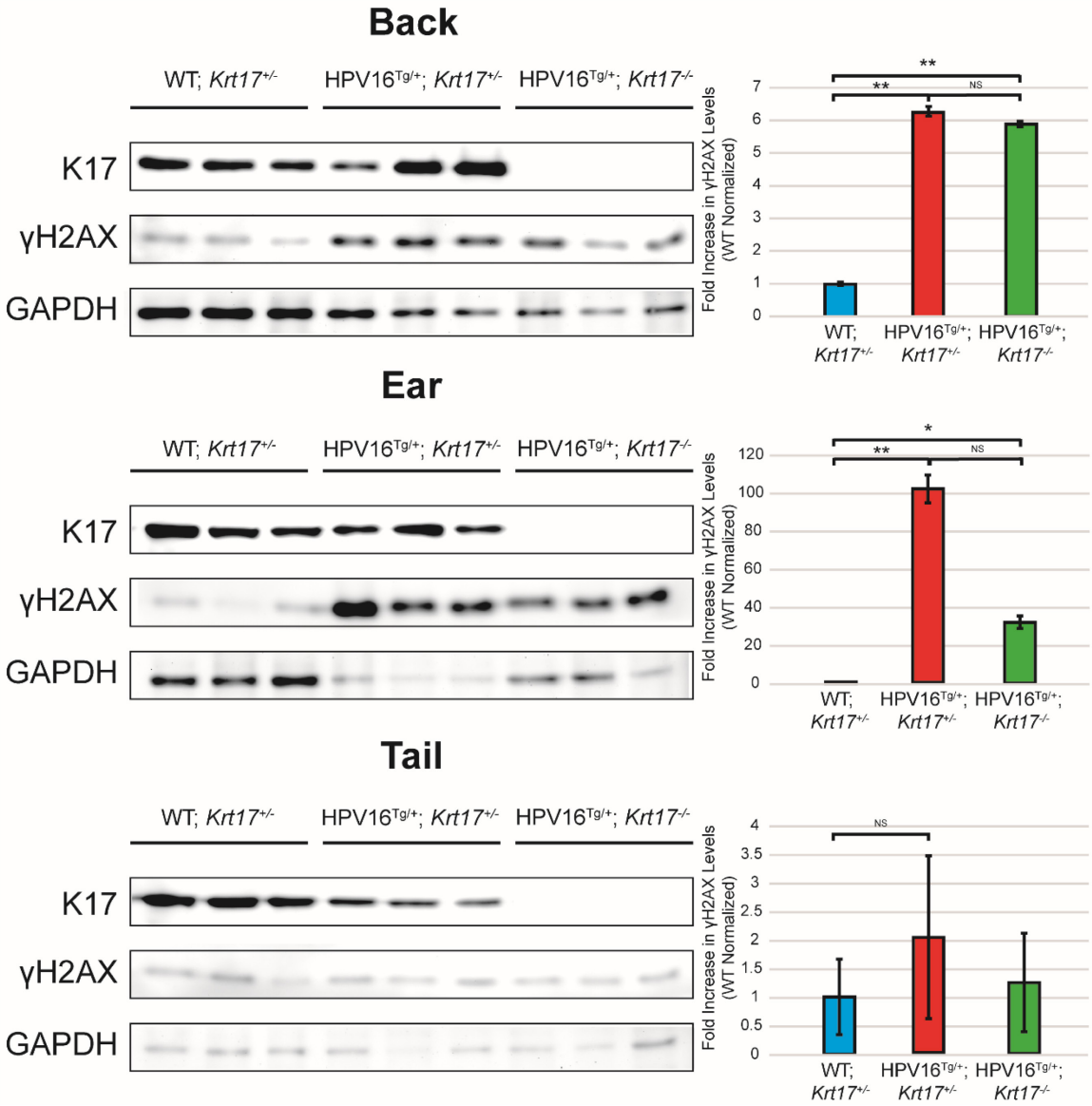

Figure 8. Elevated DNA damage is exhibited in the HPV16$^{Tg/+}$ setting compared to wild-type in female mice.

Ear, back and tail tissue was harvested from female WT K17$^{+/-}$, HPV16$^{Tg/+}$; *Krt17*$^{+/-}$ and HPV16$^{Tg/+}$; *Krt17*$^{-/-}$ mice at age P50. Protein was isolated from each sample and anti-K17, anti-γH2AX and anti-GAPDH antibodies were used to assess total protein levels. n=3 for each genotype. Error bars, s.e.m.

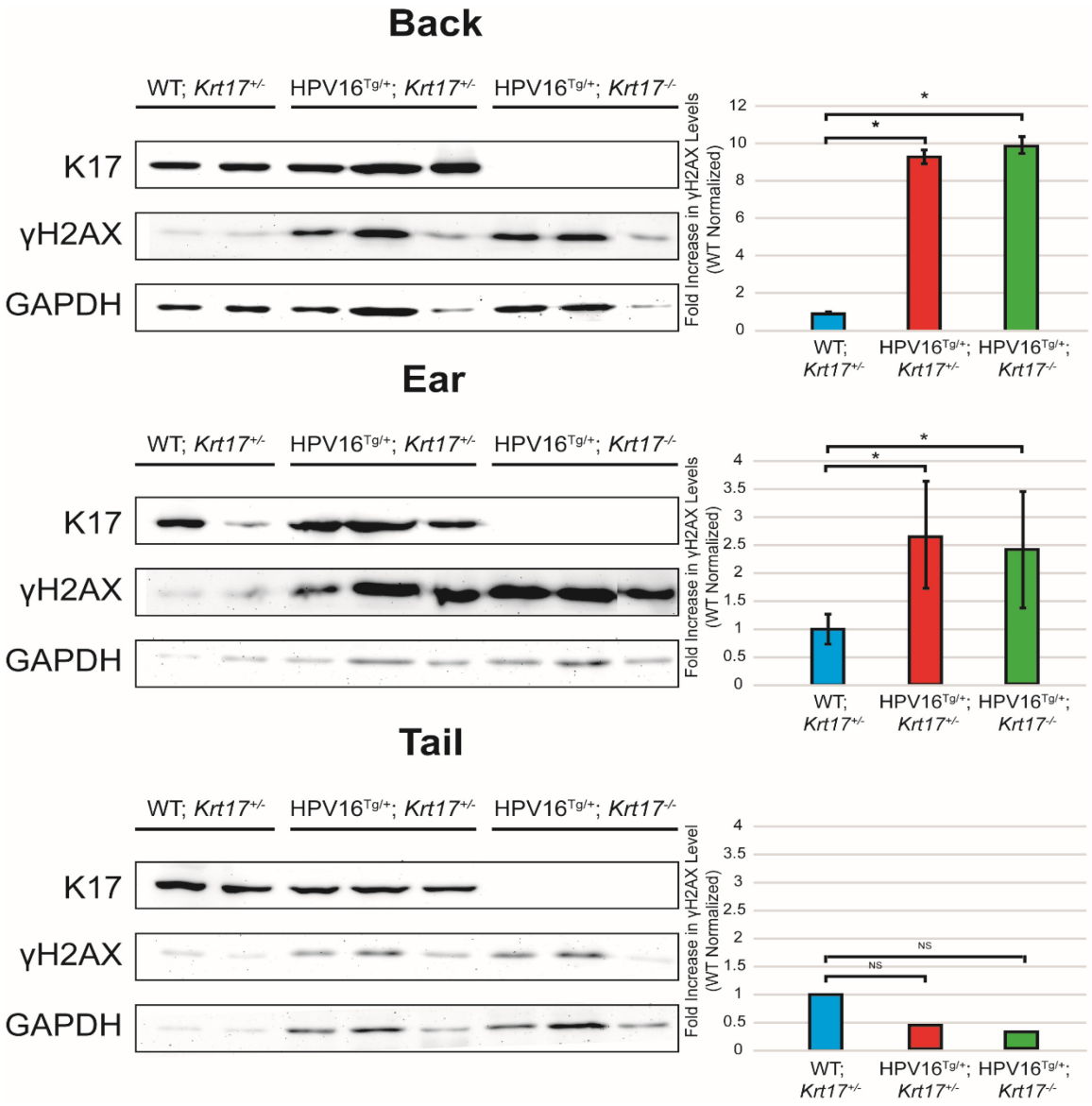

Figure 9. Elevated DNA damage is exhibited in the HPV16$^{Tg/+}$ setting compared to wild-type in male mice.

Ear, back and tail tissue was harvested from male WT K17$^{+/-}$, HPV16$^{Tg/+}$; *Krt17*$^{+/-}$ and HPV16$^{Tg/+}$; *Krt17*$^{-/-}$ mice at age P50. Protein was isolated from each sample and anti-K17, anti-γH2AX and anti-GAPDH antibodies were used to assess total protein levels. n=3 for each genotype. Error bars, s.e.m.

γH2AX-positive cells are exclusively found in the epidermis and there is no apparent dependence on K17 status

Indirect immunofluorescence microscopy for γH2AX has been used as an indicator of DNA damage in a wide variety of cancer research (Bonner *et al.*, 2008; Ivashkevich *et al.*, 2012; Qvarnström *et al.*, 2004). In order to investigate the cellular localization of γH2AX foci in murine epidermis and to substantiate the Western blot data reported above, ear, back and tail tissue was harvested from P50 male mice, snap-frozen in OCT compound, and 6-8 μm cryosections were produced. Male mice were exclusively assessed as there was no difference in the trends evident between male and female mice via immunoblot analyses, although a more exhaustive evaluation could be conducted in the future by including female mice. Sections from WT; Krt17$^{+/-}$, HPV16$^{Tg/+}$; *Krt17*$^{+/-}$ and HPV16$^{Tg/+}$; *Krt17*$^{-/-}$ mice were stained for γH2AX and total signal was quantified by averaging the pixel intensity across greater than 5 images above a threshold established by wild-type samples (n=3 biological replicates). On the basis that ear and back samples exhibited the most pronounced γH2AX signal, representative ear and back images are shown (Figure 10, 11 and 12) (tail tissue data not shown).

As observed in all three male biological replicates, γH2AX signal is found exclusively in the epidermis. The white dotted line in all reported images represents the epidermal-dermal junction and the positive cells found on the dermal side of this divide are actually in the hair follicle. This finding is in accord with the established K14-HPV16$^{Tg/+}$ model of SCC, as K14 is constitutively expressed in basal cells of the epidermis (Coulombe *et al.*, 1989; Nelson and Sun, 1983). Additionally, it appears that the highest signal, pan-nuclear stained cells are seen in the outer layers of the epidermis (Marti *et al.*, 2006).

In all three of the male biological replicates, total γH2AX intensity is higher in the HPV16$^{Tg/+}$ setting as compared to wild-type for both ear and back tissue (Figures 10, 11 and

12). In two of the three HPV16$^{Tg/+}$; *Krt17*$^{-/-}$ ear sections γH2AX levels were higher than the corresponding HPV16$^{Tg/+}$; *Krt17*$^{+/-}$ samples (Figures 10 and11). In one of the replicates, γH2AX intensity was higher in the HPV16$^{Tg/+}$; *Krt17*$^{+/-}$ ear sample, indicating some degree of variability exists in the presence or absence of K17 (Figure 12). Furthermore, back samples from the biological replicates demonstrated a similar variability, with only one set of mice displaying a significant difference between the HPV16$^{Tg/+}$; *Krt17*$^{-/-}$ and HPV16$^{Tg/+}$; *Krt17*$^{+/-}$ settings (Figure 11). Cumulatively, these results suggest there is an inherent variability in DNA damage between HPV16$^{Tg/+}$; *Krt17*$^{+/-}$ and HPV16$^{Tg/+}$; *Krt17*$^{-/-}$ mice, with no apparent correlation to K17 status.

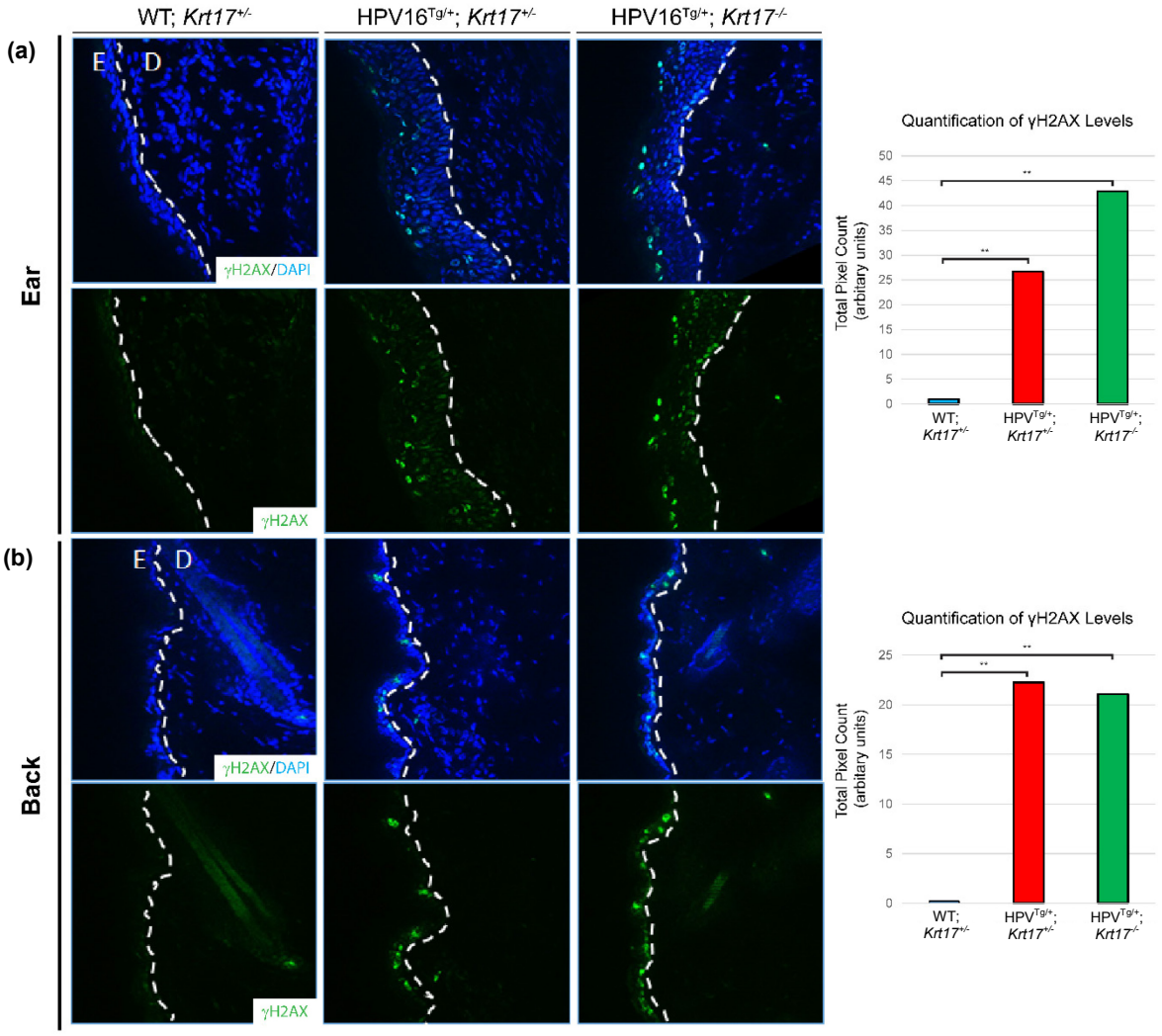

Figure 10. γH2AX levels in HPV16$^{Tg/+}$ mice vs wild-type; male biological replicate 1. Immunofluoresence microscopy images for (a) ear tissue and (b) back tissue (6-8 µm thickness). Top panel costained for DAPI and γH2AX. Bottom panel is the single channel for γH2AX. From left to right for both (a) and (b): WT; Krt17$^{+/-}$, HPV16$^{Tg/+}$; *Krt17*$^{+/-}$ and HPV16$^{Tg/+}$; *Krt17*$^{-/-}$ genotypes. E= epidermis, D= dermis; white dotted line separates epidermis and dermis. Quantification of γH2AX levels normalized to wild-type in the right hand panel.

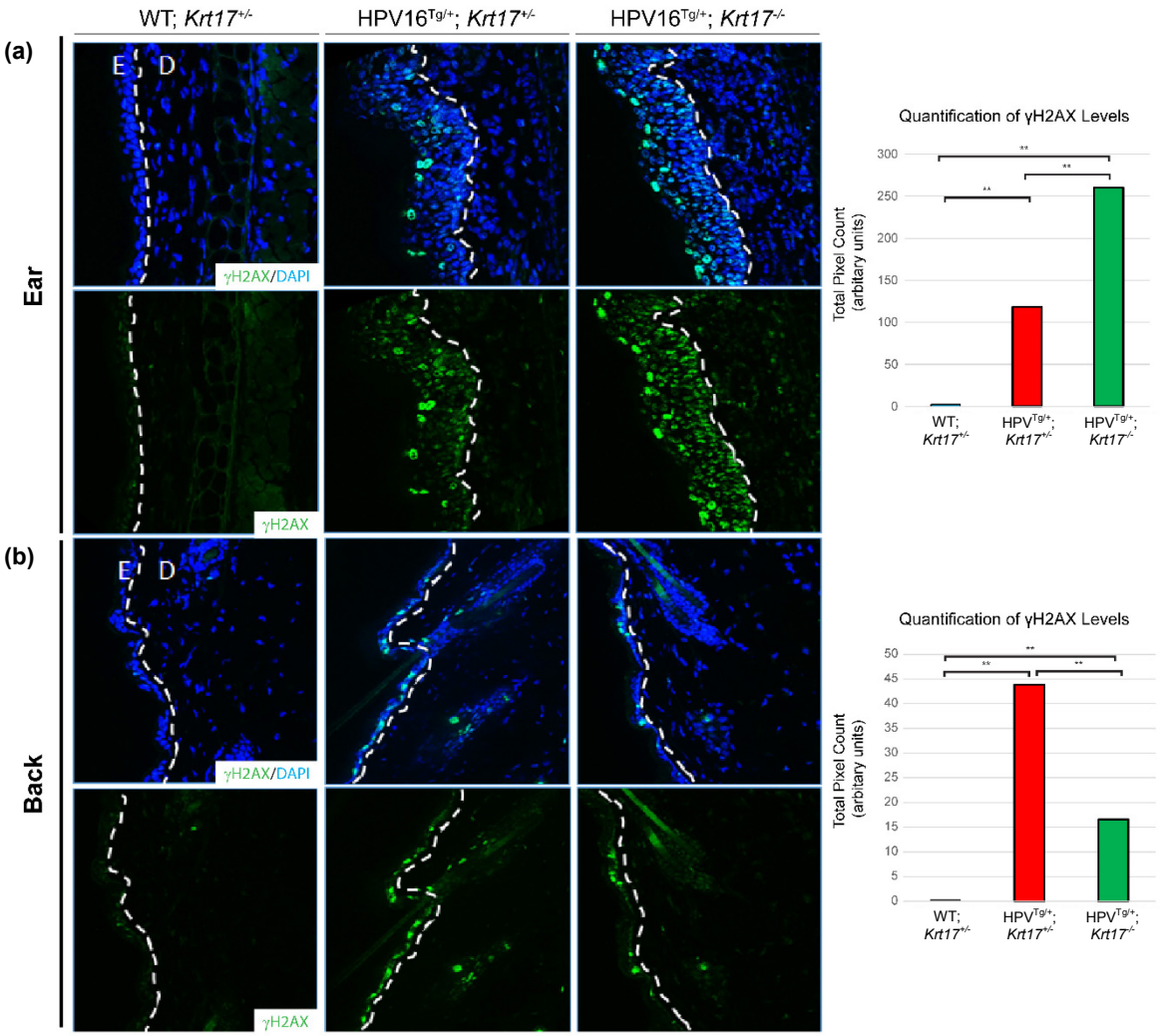

Figure 11. γH2AX levels in HPV16$^{Tg/+}$ mice vs wild-type; male biological replicate 2.
See Figure 10.

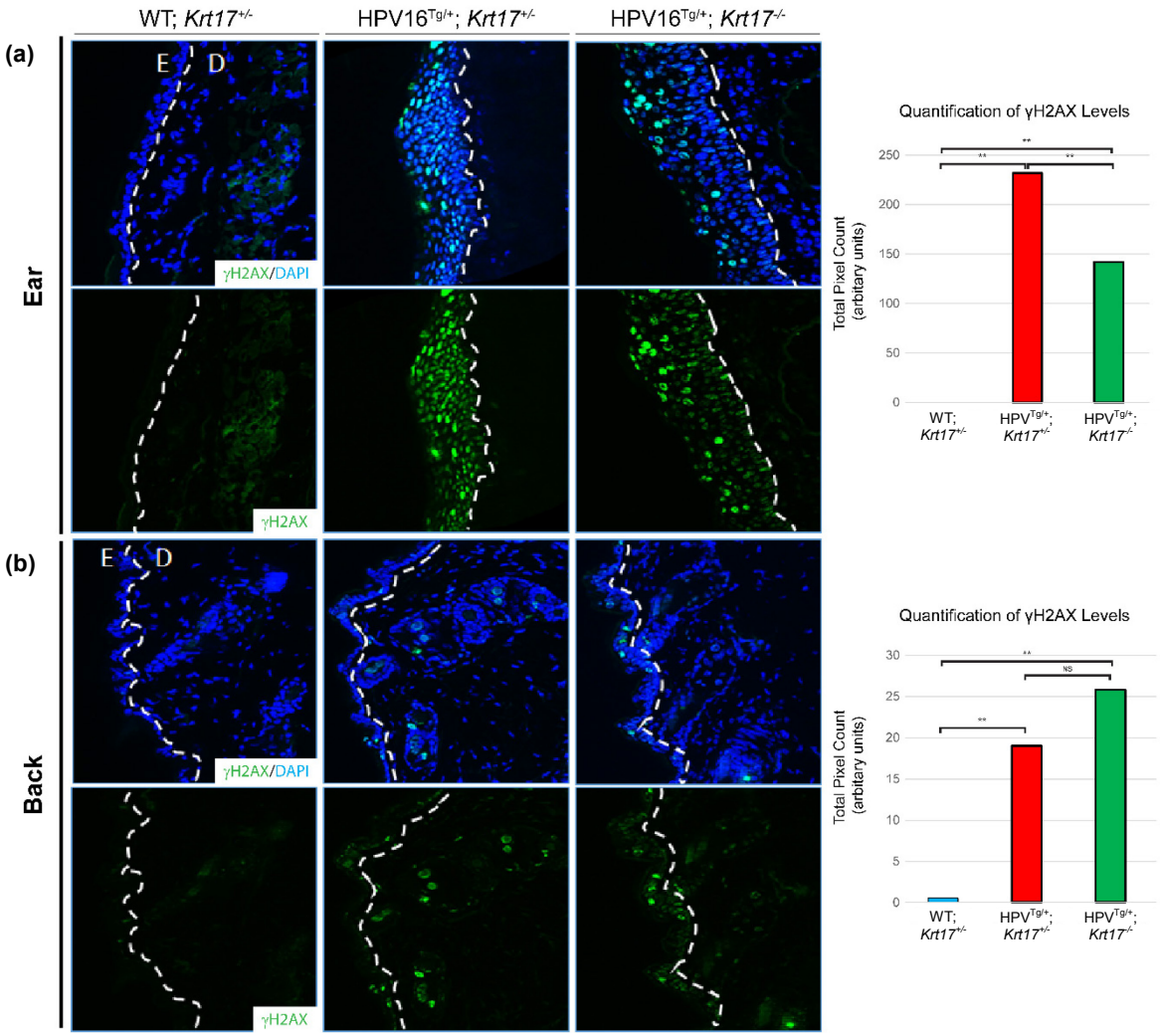

Figure 12. γH2AX levels in HPV16$^{Tg/+}$ mice vs wild-type; male biological replicate 3.
See Figure 10.

A tissue specific gradient is established in both male and female mice for the HPV16$^{Tg/+}$ model

Ear tissue of the K14-HPV16$^{Tg/+}$ mouse line is well documented as the most consistently affected site by squamous cell carcinoma lesions (Arbeit and Hanahan, 1994). Additionally, substantial research has been conducted on this model in a variety of other tissues, including cervical epithelium and oral epithelium, among others (Hobbs *et al.*, 2016; Sdek *et al.*, 2006).

To test whether the extent of DNA damage varies by tissue site, we directly compared by Western blotting ear, back and tail protein isolates in triplicate and separated by genotype. Herein, we define a tissue specific gradient in both the HPV16$^{Tg/+}$; *Krt17*$^{+/-}$ and HPV16$^{Tg/+}$; *Krt17*$^{-/-}$ settings, but not in WT; *Krt17*$^{+/-}$ mice. In female HPV16$^{Tg/+}$; *Krt17*$^{+/-}$ mice, as would be expected, ear tissue exhibited the most significant amount of DNA damage, followed by back and tail tissue (Figure 13). Due to the fact that tail tissue exhibited the lowest level of total γH2AX, ear and back isolates were normalized to tail and displayed as a fold increase. In HPV16$^{Tg/+}$; *Krt17*$^{+/-}$ mice, the gradient Ear>Back>Tail was statistically significant across all comparisons (Ear:Back, p=0.003; Ear:Tail, p=0.003; Back:Tail, p=0.03) (Figure 13, middle panel). Similarly, in HPV16$^{Tg/+}$; *Krt17*$^{-/-}$ mice, this discordance was also significant (Ear:Back, p=0.002; Ear:Tail, p=0.001; Back:Tail, p=0.04) (Figure 13, lower panel). Although a comparable pattern was seen in the respective male analyses, no statistical significance was reported, in part due to the reduced sample size and consequent reduced power (Figure 14). However, both HPV16$^{Tg/+}$; *Krt17*$^{+/-}$ and HPV16$^{Tg/+}$; *Krt17*$^{-/-}$ male mice exhibited this trend (Figure 14, middle and lower panels).

Both male and female biological replicates were pooled in order to ascertain whether this trend remained true across both sexes. Accordingly, pooled data sets were analyzed and

in both HPV16$^{Tg/+}$ settings this Ear>Back>Tail gradient was apparent (Figure 15). For HPV16$^{Tg/+}$; *Krt17*$^{+/-}$ mice: Ear:Back, p=0.014, Ear:Tail, p=0.007 and Back:Tail, p=0.029. For HPV16$^{Tg/+}$; *Krt17*$^{-/-}$ mice: Ear:Back, p=0.0007, Ear:Tail, p=0.0002 and Back:Tail, p=0.16. These data suggest that additional skin sites exhibit DNA damage in a gradient dependent manner as a result of the K14 driven-HPV16 transgene, albeit to a lesser extent than ear tissue.

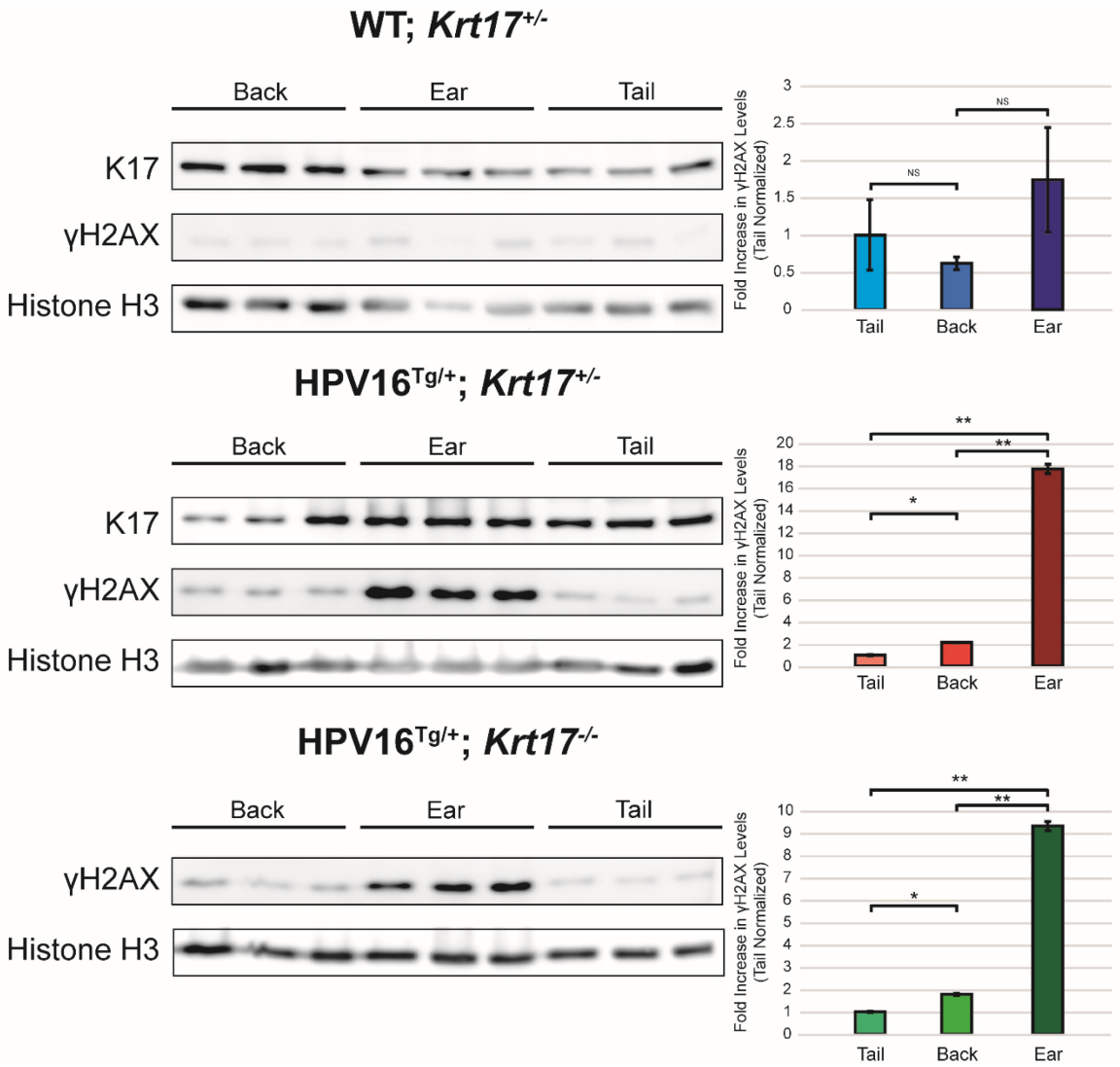

Figure 13. Tissue discordance in γH2AX levels in female mice.
Comparison of γH2AX levels across ear, back and tail tissues from each of the genotypes in female mice. Left hand panel contains Western blots from each of the three genotypes in this study. Anti-K17, anti-γH2AX and anti-Histone H3 antibodies were utilized. Right hand panel illustrates the quantification of γH2AX levels normalized to tail tissue. Error bars, s.e.m.

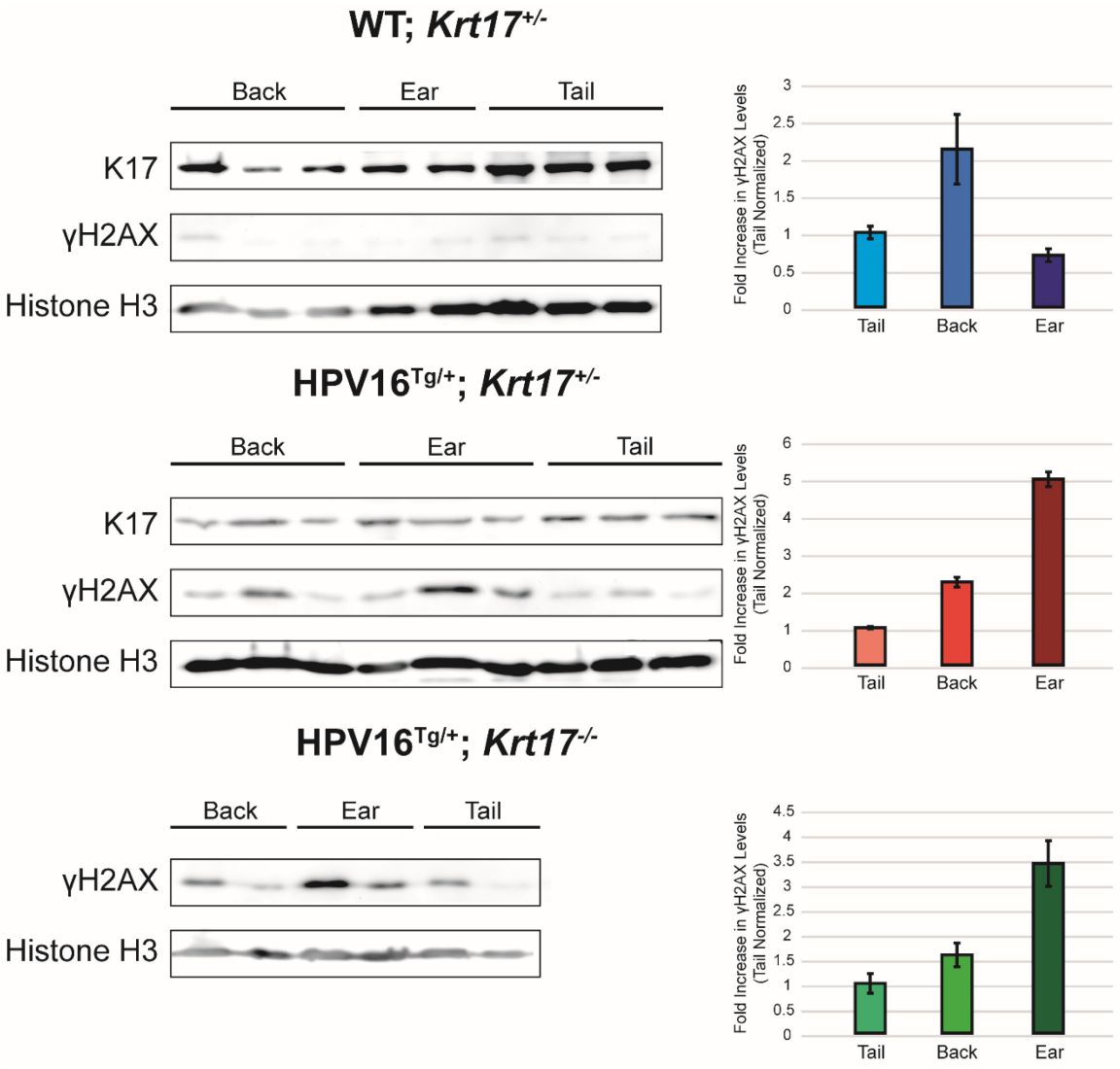

Figure 14. Tissue discordance in γH2AX levels in male mice.
Comparison of γH2AX levels across ear, back and tail tissues from each of the genotypes in male mice. Left hand panel contains Western blots from each of the three genotypes in this study. Anti-K17, anti-γH2AX and anti-Histone H3 antibodies were utilized. Right hand panel illustrates the quantification of γH2AX levels normalized to tail tissue. Error bars, s.e.m.

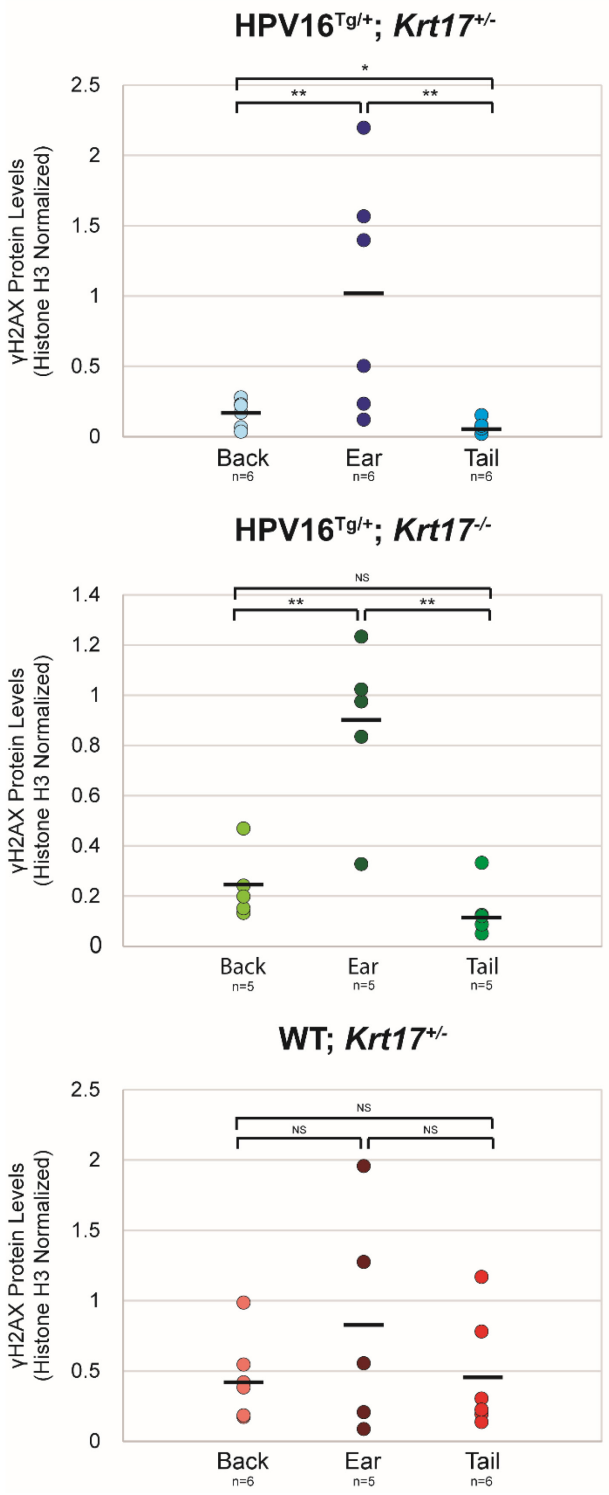

Figure 15. Tissue discordance in γH2AX levels in both male and female mice.
Pooled male and female data of γH2AX protein levels in ear, back and tail samples for WT; Krt17$^{+/-}$, HPV16$^{Tg/+}$; *Krt17*$^{+/-}$ and HPV16$^{Tg/+}$; *Krt17*$^{-/-}$ genotypes. N≥5 for all samples. Horizontal black bars indicate the average for each data set.

Quantitative RT-PCR reveals variable expression of DNA damage response elements independent of K17 status

To dissect whether the gene expression patterns of well-known DNA damage-associated proteins were altered in the presence or absence of K17, qRT-PCR assays were conducted for *Atm*, *Atr*, *Chk1*, *Chk2*, *Foxm1*, *Trp53* and *Xrcc5*. Gene expression levels were compared for ear, back and tail tissue sections across all genotypes for male and female mice (n=3 biological replicates) and values were expressed as a fold change over WT; *Krt17*$^{+/-}$ counterparts. Essentially, these findings indicate variable expression across tissue site and genotype for a number of the DNA damage-associated genes.

Qualitatively, it appears that there was higher expression of *Atm* and *Chk1* in male mice compared to females, although this was not quantitatively ascertained from the data (Figure 16, top panel). Moreover, for these two genes, no statistical significance was evident across all experimental parameters, with the exception of *Atm* in ear tissue of HPV16$^{Tg/+}$; *Krt17*$^{+/-}$ versus HPV16$^{Tg/+}$; *Krt17*$^{-/-}$ male mice ($p=0.045$).

Greater differences between WT and HPV16$^{Tg/+}$ settings were apparent in the qRT-PCR data for the *Atr* and *Chk1* targets (Figure 16, middle panels). In particular, the transcripts of both *Atr* and *Chk1* were upregulated in HPV16$^{Tg/+}$ male ears compared to wild-type ($p<0.05$ for all: See figure 16) with no significant disparity upon K17 ablation. However, this trend was only apparent in *Atm* levels in female HPV16$^{Tg/+}$; *Krt17*$^{-/-}$ back tissue ($p=0.003$), potentially as a result of inter-biological replicate variations or sex-based differences in response to DNA damaging events.

Multiple comparisons between the transgenic genotypes and wild-type mice indicated significant differences in *Foxm1* expression. *Foxm1* is a proliferation associated gene with both initiation and promotion-associated roles attributable to the protein product, FOXM1

(Wierstra and Alves, 2007). HPV16$^{Tg/+}$ male ear and back tissue exhibited elevated *Foxm1* levels compared to wild-type with no dependence on K17 status ($p<0.05$: See Figure 16, bottom panel). Similarly, HPV16$^{Tg/+}$ female back and tail tissue displayed a comparable trend, despite no differences in RNA from ear tissue.

The *Trp53* gene encoding for the P53 protein is downregulated in HPV16$^{Tg/+}$ female mice compared to wild-type across all tissue sites (statistically significant $p<0.05$ in back and tail tissue) along with male ears ($p<0.02$). This finding is unusual as it is known that the established mechanism for HPV infection involves the proteolytic degradation of P53 by the E6 oncoprotein of the HPV16 genome. Additionally, and somewhat surprisingly, we observed that *Xrcc5*, a direct target of P53, exhibited a similar downregulation in female mice ($p<0.05$) (Figure 16, bottom panel).

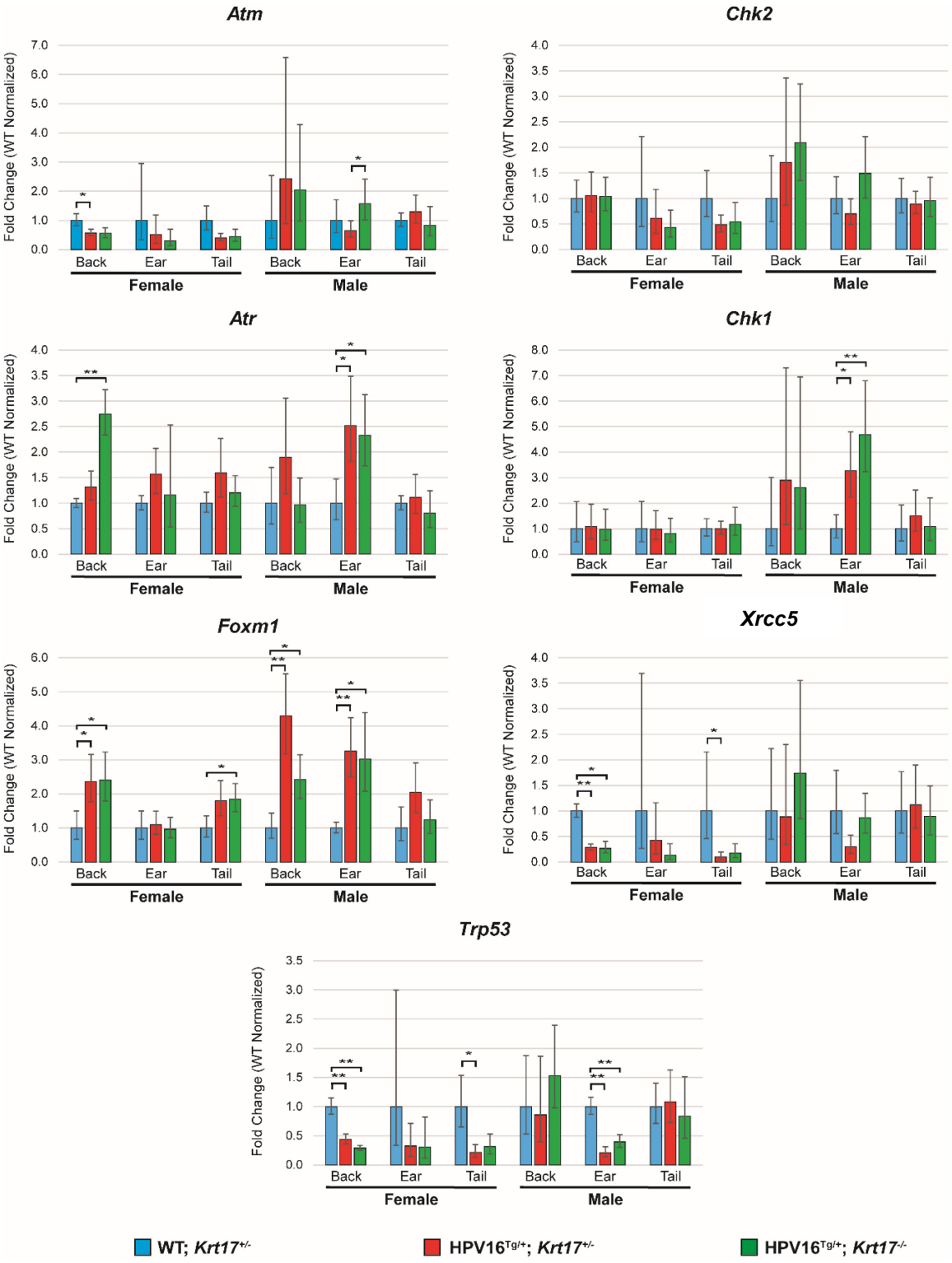

Figure 16. qRT-PCR analyses of DNA damage response-associated gene expression changes
RNA isolated from ear, back and tail tissues of WT; Krt17$^{+/-}$, HPV16$^{Tg/+}$; *Krt17*$^{+/-}$ and HPV16$^{Tg/+}$; *Krt17*$^{-/-}$ male and female mice was assessed for changes in notable DDR-associated genes. All values are exhibited as a fold change over WT. *P<0.05; **P<0.02. Error= upper and lower limit of standard error.

K17 appears to be induced upon treatment with the mutagen, DMBA, compared to control

DMBA, a polycyclic aromatic hydrocarbon, is a potent carcinogen that is known to have deleterious effects on DNA after systemic exposure, forming a wide variety of DMBA-DNA adducts (Dipple *et al.*, 1984; Slaga *et al.*, 1974; Ward *et al.*, 1986). Specifically, DMBA frequently induces an activating A to T transversion in codon 61 of the *Hras1* gene, a notable oncogene (Brown *et al.*, 1990). Moreover, DMBA is a commonly utilized initiating agent in two-step chemical carcinogenesis experimental protocols (Abel *et al.*, 2009).

As a means of determining whether K17 is induced upon acute DNA damage, male mice were administered either 100 μg DMBA (in 200 μl of acetone vehicle) or 200 μl of acetone control via intraperitoneal (IP) injection and back tissue sections were harvested 7 days later. Indirect immunofluorescence microscopy images stained for both K17 and γH2AX suggest that γH2AX expression is induced upon treatment with DMBA compared to acetone control (Figure 17, lower panels). More promisingly, K17 levels appear to be elevated in the treated male mice compared to control (Figure 17, upper panels). This finding, although preliminary, suggests that K17 may play a role in the initiating events of acute DNA damage.

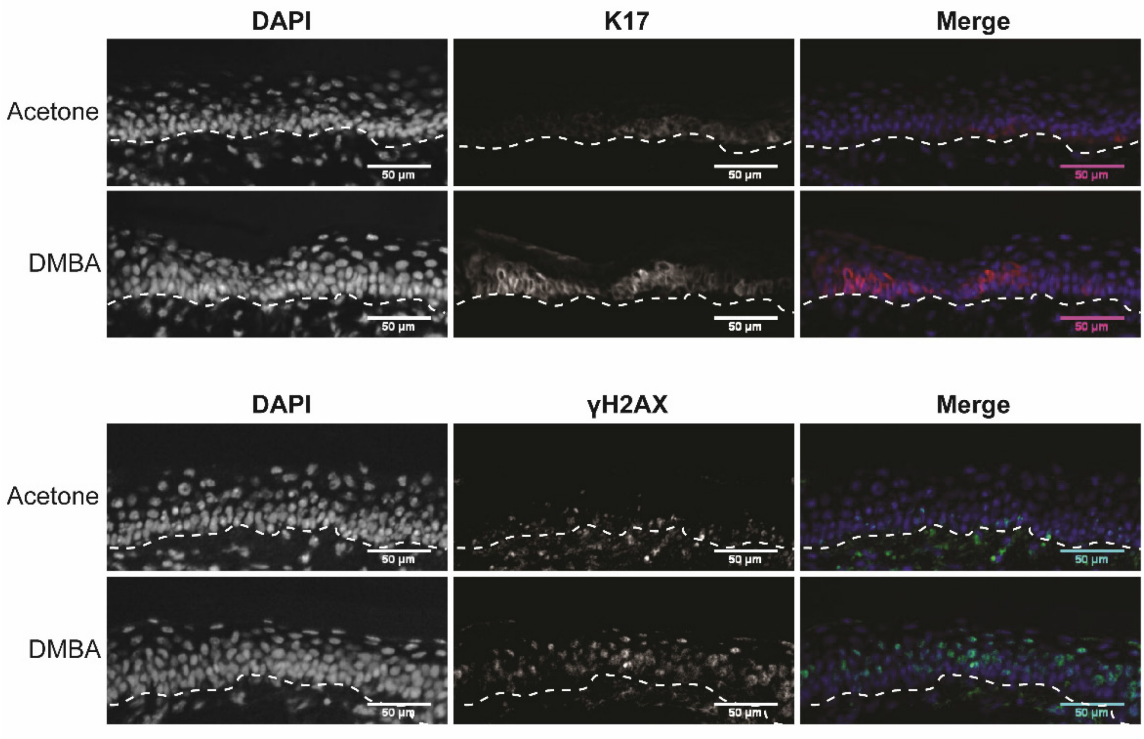

Figure 17. K17 may be induced upon systemic treatment with the mutagen, DMBA. Six-week-old male mice IP injected with either 100µg DMBA (200 µl volume) or acetone (200 µl volume) and back tissue harvested and embedded in OCT one week later. Top panel depicts K17 staining and bottom panel illustrates γH2AX staining in acetone versus DMBA injected mice. Scale bars, 50 µm. Figure from R. Hobbs, 2015.

DISCUSSION

The research described in this thesis uncovers new details regarding the HPV16$^{Tg/+}$ model for SCC in addition to offering preliminary insight about the relationship between K17 and DNA damage.

Stemming from the extensively reported observations that K17 is induced in a variety of stress/inflammatory settings, and coupled with the knowledge that K17 directly impacts the course of tumorigenesis through a number of mechanisms, we set out to elucidate whether K17 plays a role in response to an acute challenge with a DNA mutagen. This acute model is a particularly logical and appropriate context since it draws upon the inducible nature of K17 and provides a definitive window that parallels the initiation stage of carcinogenesis. Our preliminary findings indicate that the systemic treatment of the mutagen, DMBA, elicits an upregulation of K17 concurrent with elevated DNA damage in murine back tissue, as represented by γH2AX staining. Notably, K17 induction appears to be localized to the basal layer, which contains the most proliferative cells of the epidermis (Potten, 1974). As DNA damage is an initiating event, and the clonal expansion of initiated cells is necessary for the eventual development of tumors, the contemporaneous elevation of K17 and γH2AX levels in the basal layer suggests that K17 may play a role in the initiating events of carcinogenesis.

Conversely, the properties of DMBA and its cellular effects may in fact pose a more significant complication than initially thought when ascertaining K17 involvement in initiation versus promotion stages. Prior *in vivo* studies of DMBA have identified a number of additional effects, in addition to DNA adduct formation. Using common inflammatory (i.e. tumor promotion) experimental readouts including edema, hyperplasia and polymorphonuclear leukocyte infiltrates (measured by MPO), Frenkel *et al.* (1995) demonstrated that there was

substantial overlap between the physiological effects of DMBA and TPA. Furthermore, for both the MPO assay and detection of edema, DMBA treatment led to a more prolonged elevation in levels compared to TPA treatment. DMBA treatment resulted in oxidative effects and stimulated a similar inflammatory profile to that of the promoting agent, TPA, highlighted by the production of hydrogen peroxide (Frenkel *et al.*, 1995). Coincidentally, previous research in the Coulombe laboratory showed that K17 is phosphorylated on Serine 44 in response to hydrogen peroxide-induced oxidative stress, an event that modulates protein-protein interactions and downstream K17-mediated signaling events (Pan *et al.*, 2011). This may attribute what is a supposed DMBA-induced response to already established functional roles of K17 as opposed to the oncogenic event itself.

To further substantiate these observations, a number of experimental factors could be optimized in future studies. The current data presented in this thesis is from a study of one DMBA-treated and one acetone-treated mouse. A more robust sample size would solidify whether K17 induction occurs in a statistically significant manner. Additionally, the route of DMBA administration chosen was IP injection. Considerable research conducted on the two-step chemical carcinogenesis model has traditionally implemented topical DMBA treatments, although IP injections are also an effective method (DiGiovanni, 1992; Ward *et al.*, 1986). Accordingly, ascertaining the comparative DNA damage in this model as a consequence of systemic or topical treatments could prove fruitful for future work.

Another parameter that deserves further attention is the time point at which tissue is harvested after DMBA treatment. In this study, mice were treated and tissue was harvested 7 days later. The reasoning behind this was that a broader analysis of putative K17 induction upon DNA damage would be followed by more stringent time points to definitively narrow down when K17 may be switched on. The discrepancy between the rapid phosphorylation of

H2AX to γH2AX (some studies indicating it occurs as quickly as 3-10 minutes after IR exposure) and the harvest time point does permit substantial variation in K17 levels to occur if the induction is transient (Rothkamm and Horn, 2009). To this effect, what may prove useful are *in vitro* assays to narrow down the window in which K17 induction may occur in response to DMBA, due to less susceptibility to inter-biological replicate variations and their relative ease. Such studies are currently in progress in the Coulombe laboratory.

In order to complement the acute model for investigating K17 involvement in DNA damage in skin, the HPV16$^{Tg/+}$ mouse was used as a corollary for the 'chronic' development of tumors (specifically SCC) in epidermal tissue. Two principal pieces of information were used in the experimental design: 1) K17 is robustly induced in the interfollicular epidermis of HPV16$^{Tg/+}$ mice between P20 and P40 and 2) SCC lesion development arises at P60 with complete penetrance by P120 (Hobbs *et al.*, 2015). Hence, the P50 time point is considered pre-lesional and is analogous to the initiation stage of carcinogenesis. This research proposes that the presence of K17 does not impact the extent of DNA damage in mouse skin from any tissue site sampled, namely ear, back and tail. As a validation of this experimental design, there is a stark difference in γH2AX levels between wild-type and the transgenic model, reinforcing these findings. Furthermore, these observations held true for both of the most afflicted tissues, ear and back.

A closer examination of the Western blot data for female mice does suggest that there is a difference in γH2AX signal between HPV16$^{Tg/+}$; *Krt17*$^{-/-}$ and HPV16$^{Tg/+}$; *Krt17*$^{+/-}$ mice, although not statistically significant (P=0.06). This particular observation could benefit from an increased sample size (n=3 biological replicates in this data set) to determine whether the decrease in γH2AX signal in HPV16$^{Tg/+}$; *Krt17*$^{-/-}$ female mice would be of biological significance. Moreover, this finding, despite lacking statistical significance, appears to be

somewhat divergent from the more concrete male data that does not indicate K17-dependent DNA damage. Substantial efforts focused on other inducible keratins (K16 in particular) in the Coulombe laboratory have revealed sex-based differences in a variety of disease settings, most notably PC (unpublished data). Thus, a sex-based variance in DNA damage may explain the discrepancy in the male and female data sets.

What is apparent from the analysis of the immunofluorescence microscopy images is that there appears to be some degree of variability in γH2AX expression levels across biological replicates. In particular, for two of the three replicates, HPV16$^{Tg/+}$; *Krt17*$^{-/-}$ ear tissue had more γH2AX-positive cells than the HPV16$^{Tg/+}$; *Krt17*$^{+/-}$ counterparts, largely confirmed by Western blotting. This variability could extend from the fact that there is inherent variation in tumor onset and thus pinpointing the exact times at which oncogenic insults occur in pre-lesional tissue of HPV16$^{Tg/+}$ mice may prove temporally difficult (Hobbs *et al.*, 2015). Alternatively, this model does not account for potential inherent differences in mutational load between biological replicates and thus differences in γH2AX signal between HPV16$^{Tg/+}$; *Krt17*$^{-/-}$ and HPV16$^{Tg/+}$; *Krt17*$^{+/-}$ samples could be attributed to intra-strain fluctuations.

The phosphorylation of H2AX on Ser 139 is an early chromatin modification upon the initiation of DSBs during apoptosis (Rogakou *et al.*, 2000). In both of the previously used models of K17 in carcinogenesis (Gli2- BCC and K14-HPV16$^{Tg/+}$- SCC), it was reported that K17 did not impact apoptosis (DePianto *et al.*, 2010; Hobbs *et al.*, 2015). Rather, K17-driven cell proliferation was a central component of its contributions to carcinogenesis. Accordingly, the apparent localization of γH2AX-positive cells by immunofluorescence microscopy in both the HPV16$^{Tg/+}$; *Krt17*$^{-/-}$ and HPV16$^{Tg/+}$; *Krt17*$^{+/-}$ settings is most likely not indicative of apoptotic cell death. Cells in the basal layer are destined for either continued proliferation or terminal differentiation, the latter of which would provide a context for apoptosis (Cotsarelis

et al., 1990). However, in this HPV16$^{Tg/+}$setting, there are profound perturbations in terminal differentiation of keratinocytes, underscoring that the γH2AX-positive cells are a result of this particular SCC model and K17 involvement is not complicated by normal physiological processes (Arbeit *et al.*, 1994).

Future research efforts could focus on the potential for DNA damage initiating events during the period where K17 exhibits the most robust upregulation in this transgenic mouse model: P20 to P40. The limitations of *in vivo* models like the one at hand are that it becomes challenging to determine when oncogenic insults occur prior to obvious macroscopic lesion development. The transgene in the HPV16$^{Tg/+}$ mice is kicked on in embryonic development, however the 60-day window between this and lesion development is a rather large timeframe to investigate K17-dependent DNA damage. It may well be that the explanation for the previously reported strong upregulation of K17 between P20 and P40 is attributable to initiating events and that the genetic ablation of K17 in this window would be of significant biological relevance.

The increased presence of γH2AX in both HPV16$^{Tg/+}$; *Krt17*$^{-/-}$ and HPV16$^{Tg/+}$; *Krt17*$^{+/-}$ mice does not necessarily indicate that DDR effector molecules are more abundant. Indeed, protein abundance is not necessarily indicative of elevated gene expression and thus the two analyses are intended to be complementary in understanding the cellular underpinnings of carcinogenesis and other disease settings (Greenbaum *et al.*, 2003). To resolve a holistic picture of the role of K17 in DNA damage, qRT-PCR assays were run for a number of notable DDR genes. These included genes for the ATM-CHK2 and ATR-CHK1 signaling pathways, along with *Trp53*, *Foxm1* and *Xrcc5* which are distinctively upregulated in response to DNA damage (a detailed description of each can be found in Appendix A).

The ATM-CHK2 pathway is necessary for the phosphorylation of H2AX to γH2AX (Smith *et al.*, 2010). Additionally, this pathway preferentially responds to DSBs and it is known that HPV viral integration in the basal cells of the epidermis requires DSBs (Arbeit *et al.*, 1994). One may expect that the gene expression of *Atm* and *Chk2* is elevated in the HPV16$^{Tg/+}$ setting however it appears that no significant elevation occurs across both genotypes and all tissue sites sampled, with a slightly more pronounced change in males compared to females. In male ear tissue, there was a statistically significant upregulation of *Atr* and *Chk1* compared to wild-type and no discernible dependence on K17 status. As ear tissue is the most frequent site for SCC lesion development, this suggests that DNA damage is occurring prior to lesion development and K17 does not significantly attenuate or exacerbate this.

A more conclusive observation from the qRT-PCR data is that there is significant variability in gene expression between biological replicates. Additionally, the differences in DNA damage by γH2AX detection in immunofluorescence microscopy and Western blotting analyses is not entirely reflected at the transcriptional level, based on the expression of the known effectors of the H2AX to γH2AX phosphorylation event. What may explain this is that the kinase activity of ATM is increased in response to DNA damage as opposed to a substantial elevation of the *Atm* transcript (Burma *et al.*, 2001). Alternatively, the 'window' for DNA damage may occur earlier than P50 resulting in lower than anticipated transcript levels for these DDR genes.

Analyses of the *Xrcc5* and *Trp53* expression levels provides additional intriguing insight into the HPV16$^{Tg/+}$ model. The E6 oncoprotein of the HPV genome specifically targets and degrades the P53 protein product. Based on the qRT-PCR data in this thesis, it appears that the expression of *Trp53* is reduced in all tissue sites of female mice and the ear tissue of male mice, suggesting that P53 degradation is apparent, although one cannot conclusively relate the

protein and transcript data (Scheffner *et al.*, 1990). In turn this may have deleterious effects on the transcriptional activation of subsequent targets involved in the DNA damage response (Fields and Jang, 1990; Raycroft *et al.*, 1990). Downregulation of *Xrcc5* expression, a gene encoding for the Ku-related protein (Ku 80) involved in DSB repair, is evident, to some extent, in the RNA isolated from female tissue and male ear tissue for qRT-PCR analyses. This downregulation is contrary to previous reports in which an inactivating mutation of the P53 protein resulted in the modulation of *Xrcc5*, a gene normally repressed by P53 (Chao *et al.*, 2006; Taccioli *et al.*, 1994). One would expect increased *Xrcc5* in this setting as P53 is degraded by the E6 oncoprotein and, as such, enables *Xrcc5* to produce the Ku80 (X-ray repair cross-complementing protein 5) protein product involved in DSB repair. However, further complicating these observations is the recently published work that P53 directly represses transcription of K17 in the stress-related setting, radiation dermatitis, signifying that the proteolytic degradation of P53 should not alter any potential DNA-damage induction of K17 in its absence (Liao *et al.*, 2016).

One piece of evidence that may allude to the fact that K17 is more closely associated with the promotion phase of carcinogenesis as opposed to initiation, is the upregulation of the *Foxm1* gene across a number of the tissue samples in both genotypes. A prominent role of FOXM1, the protein product of the *Foxm1* gene, is in the stimulation of cell growth and proliferation by promoting G1/S and G2/M-transitions and enabling the proper execution of mitosis (Wierstra and Alves, 2007). Admittedly, FOXM1 has a dual capacity for both initiation and promotion-associated functions (Wierstra and Alves, 2007). However, this data, taken in the context of the "underwhelming" upregulation of DDR-associated genes, may be an initial clue into the exclusive role of K17 in the promotion stage of tumorigenesis.

Collectively, the qRT-PCR analyses, although admittedly somewhat variable and challenging to dissect, may provide novel information for this chronic model for studying K17 involvement in DNA damage. The fact that the early gene (E6 and E7) protein products degrade central DDR components as a means of initiating subsequent SCC lesion development, may highlight that these perturbations in DDR pathways discount the protein and/or gene expression changes of DDR elements as an applicable readout for determining the effect of K17 genetic ablation on DNA damage itself.

Lastly, a tissue-specific gradient of DNA damage in the HPV16$^{Tg/+}$ model has not yet been reported. What has been previously established is that ear tissue is the most frequently observed site for the development of SCC lesions, ultimately exhibiting full penetrance (Hobbs *et al.*, 2015). However, this study reports that tissue sites in this model are differentially affected by DNA damage in a statistically significant manner. In both male and female mice, immunoblotting revealed a hierarchy of DNA damage is established: ear>back>tail, which was not evident in the corresponding wild-type tissue samples.

An initial conclusion may be that this is due to differential cellular turnover rates in murine tissues, yet prior research has indicated that dorsal and ear skin exhibit roughly comparable rates of cell production (Potten, 1975). An alternative rationale is that ear tissue in HPV16$^{Tg/+}$ mice are characterized by progressive hyperplasia and thus a direct comparison of ear and back tissue does not fully take into account the differences in epidermal thickness. Although this is a reasonable assertion, this does not shed light on why back and tail tissue are differentially affected. Further, analyses normalizing for area (data not shown) indicate that the difference between ear and back γH2AX expression levels is largely sustained by this manipulation. Ultimately, the physiological mechanism by which SCC lesion development arises in such a striking fashion in the ear tissue of HPV16$^{Tg/+}$ mice is not understood.

Nevertheless, this research validates this well-documented phenomenon and provides evidence for the presence of DNA damage in other tissue sites.

The role of K17 in modulating the inflammatory response and promoting tumor growth in a number of different cancer settings is well established (Depianto *et al.*, 2010; Hobbs *et al.*, 2015). Despite this substantial knowledge, it is not known, functionally, how K17 might specifically contribute to the distinct stages of carcinogenesis. What extends from this body of work is that K17 appears to be upregulated in an acute, 'inducible' setting, an observation that is not seen in the HPV16$^{Tg/+}$ chronic model of DNA damage initiation. Further assessment of DDR-associated genes by qRT-PCR indicates variable expression patterns with potential insight into the HPV16$^{Tg/+}$ initiated tumorigenesis model that may prompt a closer consideration of the experimental readouts used in these studies. Additionally, new insight into the K14-HPV16$^{Tg/+}$ model for squamous cell carcinoma is put forth. Although the recurring theme of the complex nature of K17 expression and its significance is apparent, continued efforts to dissect the involvement of K17 in distinct carcinogenic properties is essential.

The findings reported in this thesis, when coupled with the body of work produced in the Coulombe laboratory and others, underscore the significant relevance of K17 in a number of disease settings. The potential role of K17 in DNA damage processes will add further impetus for the future study of K17 in the specific stages of carcinogenesis. To expand on our knowledge of K17 involvement in DNA damage, future efforts could be directed at the following: i) *in vitro* analyses that can provide further mechanistic insight, for example, whether K17 is modified in response to DNA damaging agents, ii) a more robust analysis of the timepoint at which K17 may be involved in DNA damage in the HPV16$^{Tg/+}$ model, iii) an evaluation of a potential K17-DNA damage relationship in the extant Gli2^{tg} mouse model in

the Coulombe laboratory and iv) further delineation of whether K17 is responsive to acute DNA damage events such as challenge with the mutagen, DMBA.

MATERIALS AND METHODS

Mouse Models

All experimental protocols involving mice were approved by the Johns Hopkins Institutional Animal Care and Use Committee. Genotyping for the HPV16$^{Tg/+}$ and *Krt17* alleles was conducted according to established protocols (National Cancer Institute Mouse Repository, strain 01XT3; McGowan *et al.*, 2002).

HPV Transgenic Mice

C57BL/6 *Krt17*$^{-/-}$ mice were bred to K14-HPV16 (HPV16$^{Tg/+}$) mice (FVB/N strain; obtained from the National Cancer Institute Mouse Repository, strain 01XT3) to generate HPV16$^{Tg/+}$; *Krt17*$^{-/-}$. Subsequently, HPV16$^{Tg/+}$; *Krt17*$^{-/-}$ mice were backcrossed with FVB/N mice for at least six generations. HPV16$^{Tg/+}$; *Krt17*$^{+/-}$ mice were utilized in place of HPV16$^{Tg/+}$; *Krt17*$^{+/+}$ due to morphological and phenotypic similarities between the genotypes. All mice were fed rodent chow and water *ad libitum* upon weaning. Both male and female mice for HPV16$^{Tg/+}$; *Krt17*$^{+/-}$, HPV16$^{Tg/+}$; *Krt17*$^{-/-}$ and WT; *Krt17*$^{+/-}$ genotypes were euthanized and ear, back, tail and liver samples were harvested for histology, RNA and protein isolation at P50. Mice deemed sickly by veterinary staff were excluded from this study. The sample size of mice required for this study was empirically determined from previous experience and established at $n \geq 3$. No blinding or randomization was utilized in this protocol.

DMBA and Acetone Mouse Treatments

Male WT; *Krt17*$^{+/-}$ (FVB/N) mice were IP injected with either 100 μg DMBA (Sigma-Aldrich, St. Louis, MO, USA) in 200 μl of volume or acetone (Fischer Scientific, Fair Lawn, NJ, USA) at P40. DMBA was dissolved in acetone the morning of injections. Mice were anesthetized using short exposure to 20% isoflurane (v/v in propylene glycol) and subsequently IP injected using 1 ml 26G x 3/8 syringes (BD, Franklin Lakes, NJ, USA). Mice were housed separately based on the treatment administered and euthanized 7 days later. Back tissue was harvested from the DMBA and acetone treated mice and embedded in Tissue-Tec OCT compound (Sakura Finetek, Torrance, CA, USA).

Tissue Collection and Histology

Ear, back, tail and liver tissues were harvested from three to four mice for each genotype (HPV16$^{Tg/+}$; *Krt17*$^{+/-}$, HPV16$^{Tg/+}$; *Krt17*$^{-/-}$ and WT; *Krt17*$^{+/-}$) and sex in the HPV16$^{Tg/+}$ setting. Back tissue was harvested for the male WT; *Krt17*$^{+/-}$ DMBA and acetone treated mice. All tissue sections were quickly embedded in Tissue-Tec OCT compound (Sakura Finetek, Torrance, CA, USA) and stored at -20°C prior to sectioning. Tissue sections were cut at 6-8 μm in thickness and subsequently subjected to histological stains.

Protein and RNA Isolation

The four tissues harvested from the HP16$^{Tg/+}$ mice, as indicated above, were prepared for RNA, DNA and protein isolation using Trizol reagent (Invitrogen, Carlsbad, CA, USA). Tissue was homogenized for >5 minutes and directly underwent phase separation. Protein, RNA and DNA were isolated for each sample as directed by the manufacturer's protocol.

Protein lysates were prepped for Western blotting in urea sample buffer (8 M deionized urea, 0.5% SDS, 30 mM Tris, pH 6.8, 5% glycerol and 5% β-mercaptoethanol). All samples were sheared using progressively thinner gauged needles (18, 20, 22 ½, 25 ½ and 26 ½). Concentration for protein lysates was determined using an amido black assay and biophotometer (Eppendorf, Hamburg, Germany). RNA purity and concentration measurements were obtained using a nanodrop spectrophotometer (Implen, München, Germany).

Antibodies

The primary antibodies used in these studies included rabbit polyclonal antibodies against Krt17 (developed in-house; 5th bleed), histone H3 (Cell Signaling #9715, Danvers, MA, USA), normal rabbit IgG (Santa Cruz Biotechnology sc-2027, Dallas, TX, USA) and phospho-γH2AX (Cell Signaling #9718, Danvers, MA, USA); mouse polyclonal antibodies against GAPDH (Santa Cruz Biotechnology sc-365062, Dallas, TX, USA). Secondary antibodies included ones conjugated to Alexa Fluor 488 (Abcam, Cambridge, UK) for indirect immunofluorescence and horseradish peroxidase (HRP)-conjugated goat anti-mouse and goat anti-rabbit antibodies (Sigma-Aldrich, St. Louis, MO, USA) for chemiluminescence immunoblotting. 4',6-Diamidine-2'-phenylindole dihydrochloride (DAPI) (Roche 10236276001, Mannheim, Germany) was used as a nuclear marker for indirect immunofluorescence. All antibodies were used according to the manufacturer's recommendation.

Western Blotting, Indirect Immunofluorescence and Microscopy

All samples were loaded at 10-20μg of protein per lane for immunoblotting. Samples were separated using either 10% or 12.5% sodium dodecyl sulfate polyacrylamide gel electrophoresis and transferred to 0.45μm nitrocellulose membranes (Bio-Rad, Hercules, CA, USA) via a trans-blot turbo transfer system (Bio-Rad). Blots were blocked in 5% milk in PBS-T (w/v) for >1hr at room temperature (21°C) and subsequently incubated overnight at 4°C in their appropriate antibodies. Secondary antibodies were applied for 1hr at room temperature (21°C). Blots were developed using either ECL Select developing solution (GE Healthcare, Pittsburgh, PA, USA) or SuperSignal West Pico chemiluminescent substrate (Thermo Scientific, Waltham, MA, USA) and imaged using a FluorChem Q system (ProteinSimple, San Jose, CA, USA).

For indirect immunofluorescence analysis, frozen sections of the aforementioned tissues were blocked for 1hr at room temperature (21°C) in 5% normal goat serum in 1X PBS. Primary antibodies were applied overnight at 4°C. Tissue sections were imaged using a Zeiss fluorescence microscope with Apotome attachment. Images for the same marker, across all samples, genotypes and tissue types, were acquired at the same exposure, pixel range, gamma values and objective using Zen software. All images were consistently adjusted for brightness and contrast and appropriately cropped for presentation purposes using ImageJ software.

Image Quantification, Graphical Analysis and Description of Statistical Methods

Signal intensity quantification for Western blots and phospho-γH2AX immunofluorescence images was performed using ImageJ software. Western blot

densitometry values were normalized to loading control (either GAPDH or histone-H3) and averaged across the value of interest (genotype or tissue type).

Indirect immunofluorescence calculations were based upon quantification of ≥5 images for each tissue, biological replicate n≥3 and genotype at 20X magnification. γH2AX intensity was restricted to the epithelium. Wild-type samples were used as a baseline for thresholding the minimum value of γH2AX intensities due to the apparent lack of γH2AX foci. The threshold value was set for each tissue and set of genotypes and applied across all subsequent images that were quantified. Graphs accompanying IF images represent the average total pixel count of γH2AX foci in the epidermis of each set of images. Error bars in immunoblot quantification represent the standard error of the mean (s.e.m.). Error bars in the quantification of immunofluorescence images represent technical error across replicate images. All *P*-values were generated using a Student's *t*-test with two-sided distribution and equal variance via Microsoft Excel. * denotes a *P*-value of <0.05; ** denotes a *P*-value of <0.02.

Quantitative RT-PCR

Isolated RNA was purified using Nucleospin RNA Clean-Up (Macherey-Nagel, Düren, Germany). RNA (1 ug) was reverse transcribed using iScript cDNA Synthesis Kit (Bio-Rad, Hercules, CA, USA). qRT-PCR was performed on the first-strand cDNA using the qPCRBIO PureGreen Mix (Next Day Science, Rockville, MD, USA). The PCR parameters for the qRT-PCR screen included incubation at 95 °C for 5 min followed by 40 cycles of 95 °C for 10 s and 60 °C for 30 s (58°C for the *Chk2* primer set). Controls with no template or no reverse transcriptase, standard curves and a melt curve were included on every PCR plate. Normalized expression values from the qRT-PCR data were calculated using Microsoft Excel

by first averaging the relative expression for each target gene $(2^{-(C_q \text{ target gene} - C_q \text{ reference gene})})$ across all three biological replicates. Error bars were derived from the standard error of the ΔC_q values ($C_{q\,\text{target}} - C_{q\,\text{reference}}$) across all biological replicates. *Actb* and *Gapdh* were used as reference genes. A list of all qRT-PCR primers used is listed in Table 1.

MOUSE		
Target	**Primer**	**Sequence (5'→3')**
Actb	Forward	GGCTGTATTCCCCTCCATCG
	Reverse	CCAGTTGGTAACAATGCCATGT
Atm	Forward	GATCTGCTCATTTGCTGCCG
	Reverse	GTGTGGTGGCTGATACATTTGAT
Atr	Forward	GAATGGGTGAACAATACTGCTGG
	Reverse	TTTGGTAGCATACACTGGCGA
Chk1	Forward	GTTAAGCCACGAGAATGTAGTGA
	Reverse	GATACTGGATATGGCCTTCCCT
Chk2	Forward	TGACAGTGCTTCCTGTTCACA
	Reverse	GAGCTGGACGAACCCTGATA
Foxm1	Forward	CTGATTCTCAAAAGACGGAGGC
	Reverse	TTGATAATCTTGATTCCGGCTGG
Gapdh	Forward	CATGTTCCAGTATGACTCCACTC
	Reverse	GGCCTCACCCCATTTGATGT
Xrcc5	Forward	ATGGCGTGGTCGGTAAATAAG
	Reverse	CCTGTCGTTGGACAAACATAGTC
Trp53	Forward	CACAGCACATGACGGAGGTC
	Reverse	TCCTTCCACCCGGATAAGATG

Table 1. Table of forward and reverse primer sequences used in qRT-PCR analyses of ear, back and tail tissue.
RNA samples obtained from WT; Krt17$^{+/-}$, HPV16$^{Tg/+}$; *Krt17*$^{+/-}$ and HPV16$^{Tg/+}$; *Krt17*$^{-/-}$ male and female mice.

REFERENCES

Abel, E. L., Angel, J. M., Kiguchi, K., & DiGiovanni, J. (2009). Multi-stage chemical carcinogenesis in mouse skin: Fundamentals and applications. *Nature Protocols, 4*(9), 1350-1362.

Aebi, U., Fowler, W. E., Rew, P., & Sun, T. T. (1983). The fibrillar substructure of keratin filaments unraveled. *The Journal of Cell Biology, 97*(4), 1131-1143.

Arbeit, J. M., Munger, K., Howley, P. M., & Hanahan, D. (1994). Progressive squamous epithelial neoplasia in K14-human papillomavirus type 16 transgenic mice. *Journal of Virology, 68*(7), 4358-4368.

Bartek, J., & Lukas, J. (2003). Chk1 and Chk2 kinases in checkpoint control and cancer. *Cancer Cell, 3*(5), 421-429.

Bednarek, A., Budunova, I., Slaga, T. J., & Aldaz, C. M. (1995). Increased telomerase activity in mouse skin premalignant progression. *Cancer Research, 55*(20), 4566-4569.

Bonnekoh, B., Huerkamp, C., Wevers, A., Geisel, J., Sebök, B., Bange, F., . . . Mahrle, G. (1995). Up-regulation of keratin 17 expression in human HaCaT keratinocytes by interferon-γ. *Journal of Investigative Dermatology, 104*(1), 58-61.

Bonner, W. M., Redon, C. E., Dickey, J. S., Nakamura, A. J., Sedelnikova, O. A., Solier, S., & Pommier, Y. (2008). γH2AX and cancer. *Nature Reviews Cancer, 8*(12), 957-967.

Bragulla, H. H., & Homberger, D. G. (2009). Structure and functions of keratin proteins in simple, stratified, keratinized and cornified epithelia. *Journal of Anatomy, 214*(4), 516-559.

Brown, K., Buchmann, A., & Balmain, A. (1990). Carcinogen-induced mutations in the mouse c-ha-ras gene provide evidence of multiple pathways for tumor progression.

Proceedings of the National Academy of Sciences of the United States of America, 87(2), 538-542.

Cai, Z., Chehab, N. H., & Pavletich, N. P. (2009). Structure and activation mechanism of the CHK2 DNA damage checkpoint kinase. *Molecular Cell, 35*(6), 818-829.

Chao, C., Wu, Z., Mazur, S. J., Borges, H., Rossi, M., Lin, T., ... & Xu, Y. (2006). Acetylation of mouse p53 at lysine 317 negatively regulates p53 apoptotic activities after DNA damage. *Molecular and cellular biology*, *26*(18), 6859-6869.

Chellappan, S., Kraus, V. B., Kroger, B., Munger, K., Howley, P. M., Phelps, W. C., & Nevins, J. R. (1992). Adenovirus E1A, simian virus 40 tumor antigen, and human papillomavirus E7 protein share the capacity to disrupt the interaction between transcription factor E2F and the retinoblastoma gene product. *Proceedings of the National Academy of Sciences of the United States of America, 89*(10), 4549-4553.

Chung, B., Rotty, J. D., & Coulombe, P. A. (2013). Networking galore: Intermediate filaments and cell migration. *Current Opinion in Cell Biology, 25*(5), 600-612.

Chung, B. M., Arutyunov, A., Ilagan, E., Yao, N., Wills-Karp, M., & Coulombe, P. A. (2015). Regulation of C-X-C chemokine gene expression by keratin 17 and hnRNP K in skin tumor keratinocytes. *The Journal of Cell Biology, 208*(5), 613-627.

Ciccia, A., & Elledge, S. J. (2010). The DNA damage response: Making it safe to play with knives. *Molecular Cell, 40*(2), 179-204.

Commo, S., & Bernard, B. A. (1997). Immunohistochemical analysis of tissue remodelling during the anagen—catagen transition of the human hair follicle.*British Journal of Dermatology*, *137*(1), 31-38.

Cotsarelis, G., Sun, T., & Lavker, R. M. (1990). Label-retaining cells reside in the bulge area of pilosebaceous unit: Implications for follicular stem cells, hair cycle, and skin carcinogenesis. *Cell, 61*(7), 1329-1337.

Coulombe, P. A., & Omary, M. B. (2002). 'Hard'and 'soft'principles defining the structure, function and regulation of keratin intermediate filaments. *Current Opinion in Cell Biology, 14*(1), 110-122.

Coulombe, P. A., & Fuchs, E. (1990). Elucidating the early stages of keratin filament assembly. *The Journal of Cell Biology, 111*(1), 153-169.

Coulombe, P. A., & Fuchs, E. (1993). Epidermolysis bullosa simplex. *Seminars in Dermatology, 12*(3), 173-190.

Coulombe, P. A., Kopan, R., & Fuchs, E. (1989). Expression of keratin K14 in the epidermis and hair follicle: Insights into complex programs of differentiation. *The Journal of Cell Biology, 109*(5), 2295-2312.

Coulombe, P. A., Miller, S.J., and Sun, T.T. "Epidermal Growth and Differentiation." Ed. Lowell A. Goldsmith. *Fitzpatrick's Dermatology in General Medicine*. By Thomas B. Fitzpatrick. Ed. Stephen I. Katz, Barbara A. Gilchrest, Amy S. Paller, David J. Leffel, and Klaus Wolff. 8th ed. Vol. 1. New York: McGraw-Hill Medical, 2012. 480-81. Print.

Coussens, L. M., & Werb, Z. (2002). Inflammation and cancer. *Nature, 420*(6917), 860-867.

de Jong, E. M., Vlijmen, I., Erp, v. P., Ramaekers, F., Troyanovski, S., & Kerkhof, P. (1991). Keratin 17: A useful marker in anti-psoriatic therapies. *Archives of Dermatological Research, 283*(7), 480-482.

DePianto, D., Kerns, M. L., Dlugosz, A. A., & Coulombe, P. A. (2010). Keratin 17 promotes epithelial proliferation and tumor growth by polarizing the immune response in skin. *Nature Genetics, 42*(10), 910-914.

DiGiovanni, J. (1992). Multistage carcinogenesis in mouse skin. *Pharmacology & Therapeutics, 54*(1), 63-128.

Dipple, A., Pigott, M. A., Bigger, C. A., & Blake, D. M. (1984). 7,12-dimethylbenz[a] anthracene--DNA binding in mouse skin: Response of different mouse strains and effects of various modifiers of carcinogenesis. *Carcinogenesis, 5*(8), 1087-1090.

Doorbar, J. (2006). Molecular biology of human papillomavirus infection and cervical cancer. *Clinical science*, *110*(5), 525-541.

Escobar-Hoyos, L. F., Yang, J., Zhu, J., Cavallo, J. A., Zhai, H., Burke, S., . . . Shroyer, K. R. (2014). Keratin 17 in premalignant and malignant squamous lesions of the cervix: Proteomic discovery and immunohistochemical validation as a diagnostic and prognostic biomarker. *Modern Pathology: An Official Journal of the United States and Canadian Academy of Pathology, Inc, 27*(4), 621-630.

Evan, G. I., & Vousden, K. H. (2001). Proliferation, cell cycle and apoptosis in cancer. *Nature, 411*(6835), 342-348.

Fields, S., & Jang, S. K. (1990). Presence of a potent transcription activating sequence in the p53 protein. *Science (New York, N.Y.), 249*(4972), 1046-1049.

Franke, W. W., Schmid, E., Osborn, M., & Weber, K. (1978). Different intermediate-sized filaments distinguished by immunofluorescence microscopy. *Proceedings of the National Academy of Sciences of the United States of America, 75*(10), 5034-5038.

Fraser, R., MacRae, T., & Rogers, G. E. (1972). *Keratins: Their composition, structure, and biosynthesis* Springfield, IL: Thomas, 1972. Print.

Frenkel, K., Wei, L., & Wei, H. (1995). 7, 12-dimethylbenz [a] anthracene induces oxidative DNA modification in vivo. *Free Radical Biology and Medicine, 19*(3), 373-380.

Fuchs, E., & Weber, K. (1994). Intermediate filaments: Structure, dynamics, function and disease. *Annual Review of Biochemistry, 63*(1), 345-382.

Fuchs, E., & Marchuk, D. (1983). Type I and type II keratins have evolved from lower eukaryotes to form the epidermal intermediate filaments in mammalian skin.

Proceedings of the National Academy of Sciences of the United States of America, 80(19), 5857-5861.

Gillespie, K. A., Mehta, K. P., Laimins, L. A., & Moody, C. A. (2012). Human papillomaviruses recruit cellular DNA repair and homologous recombination factors to viral replication centers. *Journal of Virology, 86*(17), 9520-9526.

Grachtchouk, M., Mo, R., Yu, S., Zhang, X., Sasaki, H., Hui, C., & Dlugosz, A. A. (2000). Basal cell carcinomas in mice overexpressing Gli2 in skin. *Nature Genetics, 24*(3), 216-217.

Greenbaum, D., Colangelo, C., Williams, K., & Gerstein, M. (2003). Comparing protein abundance and mRNA expression levels on a genomic scale. *Genome Biology, 4*(9), 1.

Gu, L., & Coulombe, P. A. (2007). Keratin function in skin epithelia: A broadening palette with surprising shades. *Current Opinion in Cell Biology, 19*(1), 13-23.

Hanahan, D., & Folkman, J. (1996). Patterns and emerging mechanisms of the angiogenic switch during tumorigenesis. *Cell, 86*(3), 353-364.

Hatzfeld, M., & Weber, K. (1990). The coiled coil of in vitro assembled keratin filaments is a heterodimer of type I and II keratins: Use of site-specific mutagenesis and recombinant protein expression. *The Journal of Cell Biology, 110*(4), 1199-1210.

Hobbs, R., Batazzi, A., Han, M., & Coulombe, P. (2016). Loss of keratin 17 induces tissue-specific cytokine polarization and cellular differentiation in HPV16-driven cervical tumorigenesis in vivo. *Oncogene.* doi: 10.1038/onc.2016.102.

Hobbs, R. P., DePianto, D. J., Jacob, J. T., Han, M. C., Chung, B., Batazzi, A. S., . . . Ong, S. (2015). Keratin-dependent regulation of aire and gene expression in skin tumor keratinocytes. *Nature Genetics, 47*(8), 933-938.

Hughes, B., Morris, C., Cunliffe, W., & Leigh, I. (1996). Keratin expression in pilosebaceous epithelia in truncal skin of acne patients. *British Journal of Dermatology, 134*(2), 247-256.

Ide, M., Kato, T., Ogata, K., Mochiki, E., Kuwano, H., & Oyama, T. (2012). Keratin 17 expression correlates with tumor progression and poor prognosis in gastric adenocarcinoma. *Annals of Surgical Oncology, 19*(11), 3506-3514.

Ivashkevich, A., Redon, C. E., Nakamura, A. J., Martin, R. F., & Martin, O. A. (2012). Use of the γ-H2AX assay to monitor DNA damage and repair in translational cancer research. *Cancer Letters, 327*(1), 123-133.

Kerns, M. L., Hakim, J. M., Lu, R. G., Guo, Y., Berroth, A., Kaspar, R. L., & Coulombe, P. A. (2016). Oxidative stress and dysfunctional NRF2 underlie pachyonychia congenita phenotypes. *The Journal of Clinical Investigation, 126*(6)

Kim, S., Wong, P., & Coulombe, P. A. (2006). A keratin cytoskeletal protein regulates protein synthesis and epithelial cell growth. *Nature, 441*(7091), 362-365.

Kim, S., & Coulombe, P. A. (2007). Intermediate filament scaffolds fulfill mechanical, organizational, and signaling functions in the cytoplasm. *Genes & Development, 21*(13), 1581-1597.

Kitamura, R., Toyoshima, T., Tanaka, H., Kawano, S., Kiyosue, T., Matsubara, R., . . . Nakamura, S. (2012). Association of cytokeratin 17 expression with differentiation in oral squamous cell carcinoma. *Journal of Cancer Research and Clinical Oncology, 138*(8), 1299-1310.

Kurz, E. U., & Lees-Miller, S. P. (2004). DNA damage-induced activation of ATM and ATM-dependent signaling pathways. *DNA Repair, 3*(8), 889-900.

Lane, D. P. (1992). Cancer. p53, guardian of the genome. *Nature, 358*, 15-16.

Liao, C., Xie, G., Zhu, L., Chen, X., Li, X., Lu, H., . . . Yue, Z. (2016). p53 is a direct transcriptional repressor of keratin 17: Lessons from a rat model of radiation dermatitis. *Journal of Investigative Dermatology, 136*(3), 680-689.

Lin, W. W., & Karin, M. (2007). A cytokine-mediated link between innate immunity, inflammation, and cancer. *The Journal of clinical investigation*,*117*(5), 1175-1183.

Liu, Q., Guntuku, S., Cui, X. S., Matsuoka, S., Cortez, D., Tamai, K., . . . Elledge, S. J. (2000). Chk1 is an essential kinase that is regulated by atr and required for the G(2)/M DNA damage checkpoint. *Genes & Development, 14*(12), 1448-1459.

Löbrich, M., Shibata, A., Beucher, A., Fisher, A., Ensminger, M., Goodarzi, A. A., . . . Jeggo, P. A. (2010). γH2AX foci analysis for monitoring DNA double-strand break repair: Strengths, limitations and optimization. *Cell Cycle, 9*(4), 662-669.

Mah, L., El-Osta, A., & Karagiannis, T. (2010). γH2AX: A sensitive molecular marker of DNA damage and repair. *Leukemia, 24*(4), 679-686.

Markey, A., Lane, E. B., Macdonald, D., & Leigh, I. M. (1992). Keratin expression in basal cell carcinomas. *British Journal of Dermatology, 126*(2), 154-160.

Mazzalupo, S., Wong, P., Martin, P., & Coulombe, P. A. (2003). Role for keratins 6 and 17 during wound closure in embryonic mouse skin. *Developmental Dynamics, 226*(2), 356-365.

McGowan, K. M., & Coulombe, P. A. (1998). Onset of keratin 17 expression coincides with the definition of major epithelial lineages during skin development. *The Journal of Cell Biology, 143*(2), 469-486.

McGowan, K. M., Tong, X., Colucci-Guyon, E., Langa, F., Babinet, C., & Coulombe, P. A. (2002). Keratin 17 null mice exhibit age- and strain-dependent alopecia. *Genes & Development, 16*(11), 1412-1422.

McLean, W., Rugg, E., Lunny, D., Morley, S., Lane, E., Swensson, O., . . . Higgins, C. (1995). Keratin 16 and keratin 17 mutations cause pachyonychia congenita. *Nature Genetics, 9*(3), 273-278.

Moll, R., Franke, W. W., Schiller, D. L., Geiger, B., & Krepler, R. (1982). The catalog of human cytokeratins: Patterns of expression in normal epithelia, tumors and cultured cells. *Cell, 31*(1), 11-24.

Moll, R., Franke, W. W., Volc-Platzer, B., & Krepler, R. (1982). Different keratin polypeptides in epidermis and other epithelia of human skin: A specific cytokeratin of molecular weight 46,000 in epithelia of the pilosebaceous tract and basal cell epitheliomas. *The Journal of Cell Biology, 95*(1), 285-295.

Morris, R. J. (2004). A perspective on keratinocyte stem cells as targets for skin carcinogenesis. *Differentiation, 72*(8), 381-386.

Mueller, M. M. (2006). Inflammation in epithelial skin tumours: Old stories and new ideas. *European Journal of Cancer, 42*(6), 735-744.

Munoz, N., Castellsagué, X., de González, A. B., & Gissmann, L. (2006). HPV in the etiology of human cancer. *Vaccine, 24*, S1-S10.

Nelson, W. G., & Sun, T. T. (1983). The 50- and 58-kdalton keratin classes as molecular markers for stratified squamous epithelia: Cell culture studies. *The Journal of Cell Biology, 97*(1), 244-251.

Oshima, R. (2002). Apoptosis and keratin intermediate filaments. *Cell Death and Differentiation, 9*(5), 486-492.

Pallari, H. M., & Eriksson, J. E. (2006). Intermediate filaments as signaling platforms. *Science's STKE: Signal Transduction Knowledge Environment, 2006*(366), pe53. doi: stke.3662006pe53

Pan, X., Kane, L. A., Van Eyk, J. E., & Coulombe, P. A. (2011). Type I keratin 17 protein is phosphorylated on serine 44 by p90 ribosomal protein S6 kinase 1 (RSK1) in a growth- and stress-dependent fashion. *The Journal of Biological Chemistry, 286*(49), 42403-42413.

Panteleyev, A. A., Paus, R., Wanner, R., Nürnberg, W., Eichmüller, S., Thiel, R., . . . Rosenbach, T. (1997). Keratin 17 gene expression during the murine hair cycle. *Journal of Investigative Dermatology, 108*(3), 324-329.

Paulin, D., & Li, Z. (2004). Desmin: A major intermediate filament protein essential for the structural integrity and function of muscle. *Experimental Cell Research, 301*(1), 1-7.

Polo, S. E., & Jackson, S. P. (2011). Dynamics of DNA damage response proteins at DNA breaks: A focus on protein modifications. *Genes & Development, 25*(5), 409-433.

Potten, C. S. (1974). The epidermal proliferative unit: The possible role of the central basal cell. *Cell Proliferation, 7*(1), 77-88.

Potten, C. S. (1975). Epidermal cell production rates. *Journal of Investigative Dermatology, 65*(6), 488-500.

Proby, C. M., Churchill, L., Purkis, P. E., Glover, M. T., Sexton, C. J., & Leigh, I. M. (1993). Keratin 17 expression as a marker for epithelial transformation in viral warts. *The American Journal of Pathology, 143*(6), 1667-1678.

Quintanilla, M., Brown, K., Ramsden, M., & Balmain, A. (1986). Carcinogen-specific mutation and amplification of ha-ras during mouse skin carcinogenesis.

Qvarnström, O. F., Simonsson, M., Johansson, K., Nyman, J., & Turesson, I. (2004). DNA double strand break quantification in skin biopsies. *Radiotherapy and Oncology, 72*(3), 311-317.

Raycroft, L., Wu, H. Y., & Lozano, G. (1990). Transcriptional activation by wild-type but not transforming mutants of the p53 anti-oncogene. *Science (New York, N.Y.), 249*(4972), 1049-1051.

Reinhardt, H. C., & Schumacher, B. (2012). The p53 network: Cellular and systemic DNA damage responses in aging and cancer. *Trends in Genetics, 28*(3), 128-136.

Rogakou, E. P., Nieves-Neira, W., Boon, C., Pommier, Y., & Bonner, W. M. (2000). Initiation of DNA fragmentation during apoptosis induces phosphorylation of H2AX histone at serine 139. *Journal of Biological Chemistry*, *275*(13), 9390-9395.

Rothkamm, K., & Horn, S. (2009). Gamma-H2AX as protein biomarker for radiation exposure. *Ann Ist Super Sanita, 45*(3), 265-271.

Rundhaug, J. E., & Fischer, S. M. (2010). Molecular mechanisms of mouse skin tumor promotion. *Cancers, 2*(2), 436-482.

Sankar, S., Tanner, J. M., Bell, R., Chaturvedi, A., Randall, R. L., Beckerle, M. C., & Lessnick, S. L. (2013). A novel role for keratin 17 in coordinating oncogenic transformation and cellular adhesion in ewing sarcoma. *Molecular and Cellular Biology, 33*(22), 4448-4460.

Scheffner, M., Werness, B. A., Huibregtse, J. M., Levine, A. J., & Howley, P. M. (1990). The E6 oncoprotein encoded by human papillomavirus types 16 and 18 promotes the degradation of p53. *Cell, 63*(6), 1129-1136.

Schutte, B., Henfling, M., Kölgen, W., Bouman, M., Meex, S., Leers, M. P., . . . Björklund, B. (2004). Keratin 8/18 breakdown and reorganization during apoptosis. *Experimental Cell Research, 297*(1), 11-26.

Schweizer, J., Bowden, P. E., Coulombe, P. A., Langbein, L., Lane, E. B., Magin, T. M., . . . Wright, M. W. (2006). New consensus nomenclature for mammalian keratins. *The Journal of Cell Biology, 174*(2), 169-174.

Sdek, P., Zhang, Z., Cao, J., Pan, H., Chen, W., & Zheng, J. (2006). Alteration of cell-cycle regulatory proteins in human oral epithelial cells immortalized by HPV16 E6 and E7. *International Journal of Oral and Maxillofacial Surgery, 35*(7), 653-657.

Sharma, A., Singh, K., & Almasan, A. (2012). Histone H2AX phosphorylation: A marker for DNA damage. *DNA Repair Protocols*, 613-626.

Slaga, T. J., Bowden, G. T., Scribner, J. D., & Boutwell, R. K. (1974). Dose-response studies on the ability of 7,12-dimethylbenz(alpha)anthracene and benz(alpha)anthracene to initiate skin tumors. *Journal of the National Cancer Institute, 53*(5), 1337-1340.

Slaga, T. J., Budunova, I. V., Gimenez-Conti, I. B., & Aldaz, C. M. (1996). The mouse skin carcinogenesis model. *The Journal of Investigative Dermatology.Symposium Proceedings / the Society for Investigative Dermatology, Inc.[and] European Society for Dermatological Research, 1*(2), 151-156.

Smith, J., Mun Tho, L., Xu, N., & Gillespie, D. A. (2010). The ATM-Chk2 and ATR-Chk1 pathways in DNA damage signaling and cancer. *Advances in Cancer Research, 108*(C), 73-112.

Steinert, P. M., & Roop, D. R. (1988). Molecular and cellular biology of intermediate filaments. *Annual Review of Biochemistry, 57*(1), 593-625.

Sun, T., Eichner, R., Nelson, W. G., Tseng, S. C., Weiss, R. A., Jarvinen, M., & Woodcock-Mitchell, J. (1983). Keratin classes: Molecular markers for different types of epithelial differentiation. *Journal of Investigative Dermatology, 81*.

Taccioli, G. E., Gottlieb, T. M., Blunt, T., Priestley, A., Demengeot, J., Mizuta, R., ... & Jeggo, P. A. (1994). Ku80: product of the XRCC5 gene and its role in DNA repair and V (D) J recombination. *Science*, *265*(5177), 1442-1445.

Tennenbaum, T., Yuspa, S. H., Grover, A., Castronovo, V., Sobel, M. E., Yamada, Y., & De Luca, L. M. (1992). Extracellular matrix receptors and mouse skin carcinogenesis: Altered expression linked to appearance of early markers of tumor progression. *Cancer Research, 52*(10), 2966-2976.

Tibbetts, R. S., Brumbaugh, K. M., Williams, J. M., Sarkaria, J. N., Cliby, W. A., Shieh, S. Y., . . . Abraham, R. T. (1999). A role for ATR in the DNA damage-induced phosphorylation of p53. *Genes & Development, 13*(2), 152-157.

Toivola, D. M., Tao, G., Habtezion, A., Liao, J., & Omary, M. B. (2005). Cellular integrity plus: Organelle-related and protein-targeting functions of intermediate filaments. *Trends in Cell Biology, 15*(11), 608-617.

Toivola, D., Strnad, P., Habtezion, A., & Omary, M. (2010). Intermediate filaments take the heat as stress proteins. *Trends in Cell Biology, 20*(2), 79-91.

Tong, X., & Coulombe, P. A. (2006). Keratin 17 modulates hair follicle cycling in a TNFalpha-dependent fashion. *Genes & Development, 20*(10), 1353-1364.

Troyanovsky, S. M., Guelstein, V. I., Tchipysheva, T. A., Krutovskikh, V. A., & Bannikov, G. A. (1989). Patterns of expression of keratin 17 in human epithelia: Dependency on cell position. *Journal of Cell Science, 93 (Pt 3)*, 419-426.

Van De Rijn, M., Perou, C. M., Tibshirani, R., Haas, P., Kallioniemi, O., Kononen, J., . . . Köchli, O. R. (2002). Expression of cytokeratins 17 and 5 identifies a group of breast carcinomas with poor clinical outcome. *The American Journal of Pathology, 161*(6), 1991-1996.

Vogel, U., Denecke, B., Troyanovsky, S. M., Leube, R. E., & Böttger, E. C. (1995). Transcriptional activation of Psoriasis-Associated cytokeratin K17 by interferon-γ. *European Journal of Biochemistry, 227*(1-2), 143-149.

Wang, Y., Lang, H., Yuan, J., Wang, J., Wang, R., Zhang, X., . . . Liu, J. (2013). Overexpression of keratin 17 is associated with poor prognosis in epithelial ovarian cancer. *Tumor Biology, 34*(3), 1685-1689.

Ward, J. M., Rehm, S., Devor, D., Hennings, H., & Wenk, M. L. (1986). Differential carcinogenic effects of intraperitoneal initiation with 7,12-dimethylbenz(a)anthracene or urethane and topical promotion with 12-O-tetradecanoylphorbol-13-acetate in skin and internal tissues of female SENCAR and BALB/c mice. *Environmental Health Perspectives, 68*, 61-68.

Wickstead, B., & Gull, K. (2011). The evolution of the cytoskeleton. *The Journal of cell biology*, *194*(4), 513-525.

Wierstra, I., & Alves, J. (2007). FOXM1, a typical proliferation-associated transcription factor. *Biological Chemistry, 388*(12), 1257-1274.

Williams, V. M., Filippova, M., Filippov, V., Payne, K. J., & Duerksen-Hughes, P. (2014). Human papillomavirus type 16 E6* induces oxidative stress and DNA damage. *Journal of Virology, 88*(12), 6751-6761.

Yamada, S., Wirtz, D., & Coulombe, P. A. (2002). Pairwise assembly determines the intrinsic potential for self-organization and mechanical properties of keratin filaments. *Molecular Biology of the Cell, 13*(1), 382-391. doi:10.1091/mbc.01-10-0522

Yuspa, S. H., Ben, T., Hennings, H., & Lichti, U. (1982). Divergent responses in epidermal basal cells exposed to the tumor promoter 12-O-tetradecanoylphorbol-13-acetate. *Cancer Research, 42*(6), 2344-2349.

Zona, S., Bella, L., Burton, M. J., de Moraes, G. N., & Lam, E. W. (2014). FOXM1: An emerging master regulator of DNA damage response and genotoxic agent resistance. *Biochimica Et Biophysica Acta (BBA)-Gene Regulatory Mechanisms, 1839*(11), 1316-132.

APPENDIX A

Atm	ATM, ataxia telangiectasia mutated protein, is responsible for the phosphorylation of a number of downstream DDR proteins on serine or threonine residues. Upon DNA damage, this protein kinase activity is significantly increased, most notably through the phosphorylation of H2AX and the downstream CHK2 protein (Kurz and Lees-Miller, 2004).
Atr	ATR, ataxia telangiectasia and Rad3-related protein, is preferentially recruited to single-stranded DNA tracts and also functions by phosphorylating downstream proteins, specifically CHK1 and P53, which amplifies the DDR signaling pathways (Ciccia and Elledge, 2010; Tibbetts *et al.*, 1999).
Chk1	The CHK1 protein is a pivotal protein kinase in controlling cell cycle progression. It is the downstream target of ATR and is phosphorylated in response to DNA damage or replication blocks to stall the cell cycle at the G2/M checkpoint (Liu *et al.*, 2000).
Chk2	*Chk2* gives rise to a stably expressed cell cycle protein product, CHK2, which is predominantly inactive unless cells are subject to DNA damage. Its activation is prompted by ATM-mediated phosphorylation in response to DSBs. In turn, CHK2 phosphorylates the N-terminal activation domain of P53, the cell cycle transcription factor E2F1 and additional downstream targets that activate cyclin-dependent kinases (CDKs) (Bartek and Lukas, 2003; Cai *et al.*, 2009).
Foxm1	*FOXM1* is a gene that encodes for the forkhead box protein M1, a proliferation-associated transcription factor. It stimulates cell growth through the promotion of the G1/S- transition and the G2/M transition. Moreover, FOXM1 regulates the subsequent expression of a number of DNA damage sensing, mediating, signaling and repair genes (Wierstra and Alves, 2007; Zona *et al.*, 2014).
Xrcc5	The protein product of the *Xrcc5* gene, Ku80, is part of the Ku heterodimer that plays a pivotal role in the repair processes of DNA DSBs via the NHEJ pathway. Correspondingly, *Xrcc5* gene expression is significantly upregulated in response to DNA damage and interacts with the notable repair proteins, such as p53 (Chao *et al.*, 2006).
Trp53	The *Trp53* gene, the mouse equivalent of the human *TP53* gene, provides instructions for making the tumor suppressor protein, P53. P53 is a prominent DDR protein with a range of responsibilities from cell cycle arrest to regulating non-cell-autonomous interactions between damaged cells and the innate immune system (Reinhardt and Schumacher, 2012).

Table 2. Description of qRT-PCR gene targets and the roles of the encoded proteins.

STEFAN A. PRENDERGAST
Curriculum Vitae

Home Address:
56 Danielle Court
Lawrenceville, NJ 08648
Email: sprende2@jhu.edu

Laboratory Address:
615 N. Wolfe Street
Room W8030
Baltimore, MD 21205

EDUCATION

2016 **Master of Science (ScM), Laboratory of Dr. Pierre A. Coulombe, PhD**
Department of Biochemistry and Molecular Biology
Johns Hopkins Bloomberg School of Public Health, Baltimore, MD

ScM Thesis: Assessing the role of Keratin 17 in the DNA damage response *in vivo*
Supervisor: Dr. Pierre Coulombe, Ph.D.
Secondary Reader: Dr. Phil Jordan, Ph.D.

MHS Thesis: The recalcitrance of pancreatic adenocarcinoma: A role for cancer stem cells
Supervior: Dr. Terry Brown, Ph.D.
Secondary Reader: Dr. Zeeshan Rasheed, M.D., Ph.D.

2013 **Bachelor of Science (BS)**
Department of Biological Sciences
University of Notre Dame, South Bend, IN

AWARDS

2016 The Reverend Melvin B. Tuggle Inaugural Community Excellence Award 2016

2009-2011 University of Notre Dame Monogram Recipient

RESEARCH EXPERIENCE

2013 **University of Notre Dame Center for Rare and Neglected Diseases,**
South Bend, IN
Undergraduate Research

- Implemented an effective clinical database for rare diseases such as Niemann-Pick Type C
- Digitized and assessed patient medical records from the Michiana Health Information Network (MHIN) to create clinical summaries and develop natural histories for clinical practitioners

2012-2013 **University of Notre Dame Freimann Life Science Center,** South Bend, IN
Undergraduate Research

- Conducted experimental protocols to determine appropriate anesthetic regimens in both neonatal mice and *Danio rerio* for subsequent use in cancer research models

2011 **Rutgers Robert Wood Johnson Medical School Orthopaedic Research Lab**, New Brunswick, NJ
Summer Intern

- Gained valuable laboratory experience through the harvesting of tendon allografts and exposure to a variety of laboratory surgeries and bioengineering projects
- Broadened research techniques through the analysis of the mechanical properties (strength, elastic modulus, failure strain and toughness) of tendons *ex vivo* using Instron technology and SigmaStat software

SELECTED PRESENTATIONS

Prendergast, S.A. Assessing the role of Keratin 17 in the DNA damage response *in vivo*. Presented at the Johns Hopkins Bloomberg School of Public Health Department of Biochemistry and Molecular Biology Research Retreat, Baltimore, MD (2016).

Prendergast, S.A., Hobbs, R.P., Poll, B.G., Coulombe, P.A. Assessing the role of Keratin 17 in the DNA damage response *in vivo*. Presented at the Johns Hopkins Bloomberg School of Medicine Department of Dermatology Research Day, Baltimore, MD (2016).

ABSTRACTS

Fletcher, A., Stewart, K., **Prendergast, S.**, Suckow, M. Evaluation of the effect of early age anesthesia for genotyping of mice on body weight. Presented at the American Association for Laboratory Animal Science National Meeting, Baltimore, MD (2013).

VOLUNTEER/LEADERSHIP EXPERIENCE

2015-2016 **Charm City Clinic**, Baltimore, MD
Co-Director of Fundraising, Auxiliary Board Member, Case Manager

2014-2015 **Thread**, Baltimore, MD
Team Leader, Mentor